A PRELIMINARY STUDY OF THE EFFECTS OF FRONT WHEEL STEERING STABILIZERS ON VEHICLE RESPONSE CHARACTERISTICS

By

DAVID LYNN TURNEY

Bachelor of Science

Louisiana Tech University

Ruston, Louisiana

1973

Submitted to the Faculty of the Graduate College
of the Oklahoma State University
in partial fulfillment of the requirements
for the Degree of
MASTER OF SCIENCE
May, 1975

A PRELIMINARY STUDY OF THE EFFECTS OF FRONT WHEEL STEERING STABILIZERS ON VEHICLE RESPONSE CHARACTERISTICS

Thesis Approved:

Donald E. Boyd
Thesis Adviser

Harry R Sebesta

Larry D Zirkle

N N Durham
Dean of the Graduate College

ACKNOWLEDGMENTS

The aid of those who helped during this study is gratefully acknowledged. I would like to express my appreciation to Dr. Donald E. Boyd, my major adviser, for his advice, instruction and encouragement during my graduate study. My thanks are extended to Drs. H. R. Sebesta, L. D. Zirkle and Mr. L. R. Ebbesen for serving on my committee.

I would like to acknowledge Dr. Sebesta and Mr. Ebbesen also for the aid they gave me in using the DYSIMP program and the auxiliary subroutine.

The School of Mechanical and Aerospace Engineering provided a Graduate Assistantship which helped make my graduate study possible.

TABLE OF CONTENTS

LIST OF FIGURES

LIST OF SYMBOLS

a	distance from the front axle to the vehicle C.G.
b	distance from the rear axle to the vehicle C.G.
d	distance between the king pins of the vehicle
e	distance from the king pin to the center of gravity for the front wheel assembly
F_s	force applied to the steering arm
F_{xi}	braking forces acting through the tires
F_{yi}	tire side-forces
F_{zi}	normal forces acting on the tires
f	lateral distance from vehicle C.G. to point of front tire contact
h	height of vehicle C.G. above ground
i	unit vector in the forward direction from the vehicle C.G.
j	unit vector in the lateral direction from the vehicle C.G.
k	radial spring constant for stabilizer device
P_1	center of gravity for the left front wheel
P_2	center of gravity for the right front wheel
q	point of contact for the rear tire forces
$\overline{R}_o$	position vector of the vehicle C.G. for the fixed axis system
$\overline{R}_{p1}$	position vector for left front wheel C.G.
$\overline{R}_{p2}$	position vector for right front wheel C.G.
$\overline{R}_q$	position vector for right rear tire point of contact
r	yawing velocity

s	distance from front wheel C.G. to point of application for steering force
U	forward velocity of the vehicle
V	lateral velocity
W_c	vehicle weight less front wheel assemblies
W_w	weight of front wheel assembly
w	distance between the tire contact points for the rear axle
Z_1	vertical load on the front axle
Z_2	vertical load on the rear axle
α_f	front slip angle
α_r	rear slip angle
δ	front wheel angle
θ	angle of rotation for the vehicle

Subscripts

1	left front wheel
2	right front wheel
3	left rear wheel
4	right rear wheel
x	vector component in the i direction
y	vector component in the j direction

CHAPTER I

INTRODUCTION

Much research has been done in the field of automotive vehicle dynamics. These studies have employed analytical models of vehicles varying in complexity from the simple automobile to a tractor-truck pulling two trailers. Some of the previous studies have been concerned with problems related to the dynamic responses of articulated vehicles during braking. Especially important were studies applied to the analysis of tractor-semitrailers where jackknifing is a major cause of accidents.

Computer simulations of vehicle dynamics have been developed including modeling of suspension systems. Through these studies much improvement has been made in the ride qualities and cornering abilities of vehicles. Several studies have been made concerning vehicle steering systems. However, in most of the previous studies of articulated vehicles, either the models were assumed to be executing a constant turn, or instead, the front wheel angles were specified.

Because steering stabilizer devices are now becoming popular for large commercial vehicles, an investigation should be made to determine their effects on the vehicle response. Thus, the purpose of the present research was to provide a method of analysis and to evaluate the performance of these stabilizing devices.

The two major objectives of this study were:

1. to derive and solve numerically the equations of motion describing the dynamic response of a four degree-of-freedom, two-axle vehicle equipped with a front wheel steering stabilizer device.

2. make a preliminary parametric study of the effects of a spring-centered steering stabilizer on the dynamic response characteristics of a typical vehicle.

This thesis documents the research conducted to meet these objectives and summarizes some of the significant results obtained.

Although the results of this research are not directly applicable to articulated vehicles, they are useful in that

1. the feasibility of fundamental methodology is established by this study;

2. some understanding of the effects of steering stabilizers is gained;

3. these results provide a basis for comparison with special cases of more complex simulation programs to be developed in the future.

Background

The literature contains results from both analytical and experimental studies relating to the dynamic responses of vehicles. Goland and Jindra [1] treated the problem of directional stability and control of an automobile in a flat turn. The dynamic equations of motions are written for a two degree-of-freedom model. A five degree-of-freedom analog computer simulation was made [2] to predict the directional response of vehicles to torque applied to the steering wheel.

"Under-steering" and "over-steering" effects for vehicles were investigated by Ellis [3]. The response of his model was expressed in terms of primary tire coefficients to demonstrate their effects on vehicle control. For studies concerning vehicle responses to steering inputs, a driver (or steering) function was used. Several driver functions with both single and multiple feedbacks have been derived [4].

Many studies of articulated vehicles have been made and were helpful in the present research by providing the basic method of analysis. A simplified analysis was made [5] of the directional stability and control of a tractor and semi-trailer combination travelling at a constant forward speed in a steady, flat turn. The combined vehicle was treated as a linear dynamic system with three degrees-of-freedom. A similar study of a semi-trailer was made [6] in which the equations of motion were derived using a suspension simulation derived using Lagrange's Equations. In a study by Mikulcik [7], a tractor-semitrailer was modeled and both were allowed to pitch, roll, yaw, and translate. Comparisons between results using the nonlinear and linearized set of equations were made and the jackknifing phenomenon was analyzed for various steering and braking inputs. This model was extended to include vertical tire flexibility, tandem-axle suspension jacking, and tandem-axle roll steer [8].

Papers have also been written on the dynamic response of trucks pulling two trailers. The first study modeled a "dolly" and trailer (only) while executing a steady, flat turn [9]. This simulation was later extended to include two trailers and a dolly. The vehicle, assuming constant forward speed and small lateral motions, was regarded as a linear system. Two degrees-of-freedom were associated with each unit

[10]. Results of a recent analysis for double trailers showed the effects of trailer loading conditions, location of the C.G., and trailer length on the stability of the system [11].

Some experimental work has been done to obtain useful tire data. A study was made for truck tires to determine the road contact forces. Graphs of the tire lateral forces versus normal force and slip angle were shown in Reference [12]. Nordeen [13] discussed a method for mathematically representing the tire lateral forces as a function of slip angles and vertical loads.

Approach to the Problem

The vehicle modeled in this study was a tractor-truck with a single rear axle. Aerodynamic characteristics, rolling resistances, and gyro effects of the wheels were not taken into consideration. The model had four degrees-of-freedom and was constrained to move on the horizontal plane. Load shifts due to forward and lateral accelerations were accounted for in calculating the normal forces on the wheels.

A moving axis system was used with the origin fixed at the vehicle center of gravity. Application of Newton's Laws both to the body and to the wheels, together with constraint equations, yielded the equations of motion. The steering input force was applied directly to the steering arms on the wheels. Various functions were used to represent driver forces applied to the steering system. Tire side-forces were obtained using a computer subroutine and the braking forces were input as functions of time. Derivation of the equations of motion and the force diagrams are given in Chapter II.

The numerical solution to the set of equations was found using DYSIMP. Chapter III contains a discussion of the solution sequence and a simplified computer flow diagram.

After the program was verified using simple cases having known physical results, three situations were studied to determine the effects of a spring-centered steering stabilizer on response characteristics. These cases were (1) an impulse-type load (simulating running over an object or chuckhole) applied to the left front wheel, (2) a simulation of a blowout of the left front tire, and (3) a small change in the vehicle heading angle. Results from these three cases are presented in Chapter IV. The conclusions from this study are given in Chapter V.

CHAPTER II

FORMULATION OF THE EQUATIONS

Equations of Motion

The equations of motion were derived considering the vehicle to be moving in a plane parallel to the horizontal road surface. Therefore, the three degrees-of-freedom associated with rigid body motion of the vehicle body are (1) forward translation, (2) lateral translation, and (3) rotation about the vehicle center of gravity. Because the front wheel rotation about the king pin axis is not prescribed, this creates a fourth degree-of-freedom for the front wheel masses.

A moving coordinate system was used with the origin attached to the vehicle center of gravity. Newton's Laws of Motions were applied to the body and to the front wheels independently. These equations were then combined through constraint equations to yield the equations of motion for the vehicle.

The body-centered axis system is shown in Figure 1. Figure 2 illustrates the moving axis system fixed to the vehicle. Differentiation of the position vector $\bar{R}_0$ twice with respect to time results in the acceleration of point O in the direction of the unit vectors i and j, and is expressible as

$$\ddot{\bar{R}}_0 = \bar{a}_0 = (\dot{U} - V \cdot r)i + (\dot{V} + U \cdot r)j$$

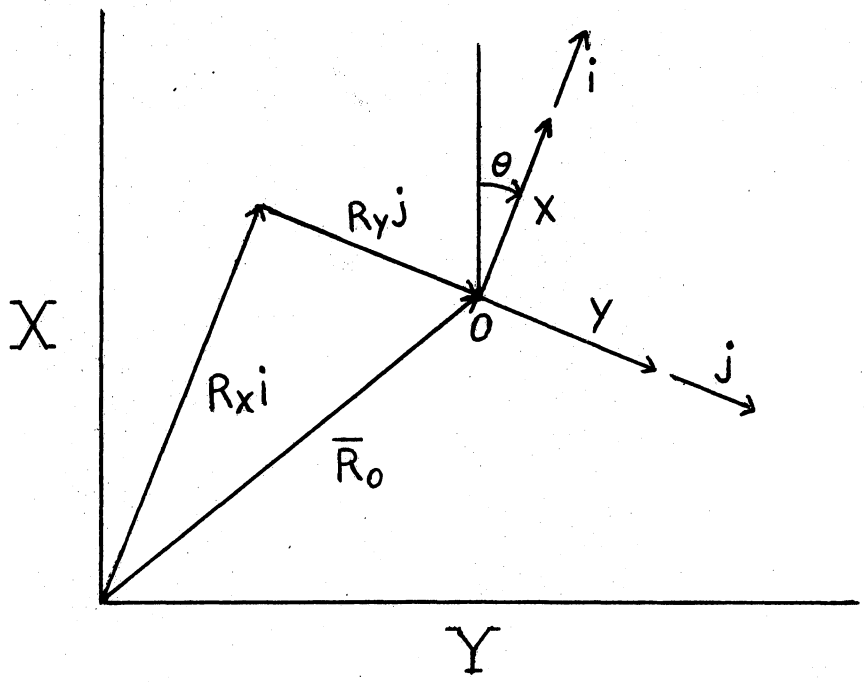

Figure 1. Body Axis System Referenced to Fixed Axis System

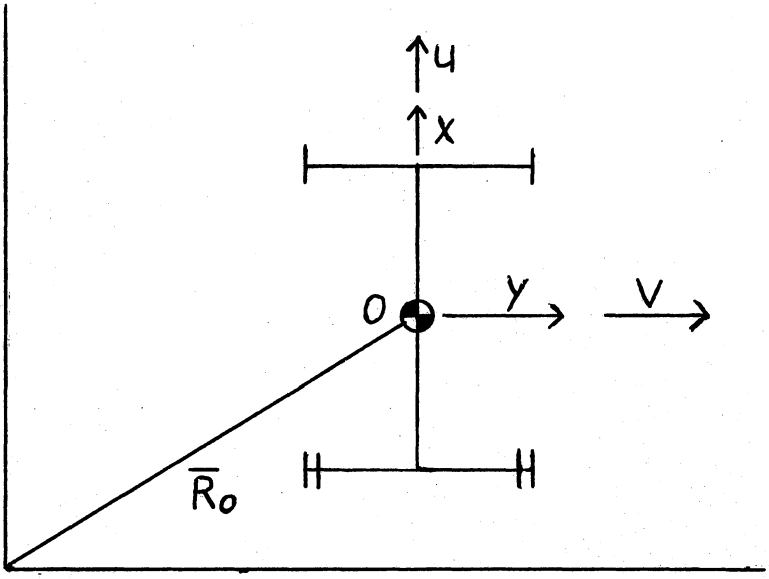

Figure 2. Moving (Body) Axis System Referenced to the Vehicle

where

$$U = \dot{R}_x - R_y\dot{\theta};$$
$$V = \dot{R}_y + R_x\dot{\theta};$$
$$r = \dot{\theta}.$$

Reference should be made to Appendix A for a complete development of the expression for $\ddot{\bar{R}}_0$. Using $\ddot{\bar{R}}_0$ the equations of motion for the vehicle shown in Figure 2 become

$$m(\dot{U} - V\cdot r) = \Sigma F_x \tag{1}$$

$$m(\dot{V} + U\cdot r) = \Sigma F_y \tag{2}$$

$$I\cdot\dot{r} = \Sigma M_0 \tag{3}$$

The horizontal forces which act on the vehicle are shown in Figure 3. In this diagram the steering angle (δ) is shown as are the steering input forces, F_{s1} and F_{s2}. Tire side-forces are denoted by F_{yi} and are acting perpendicular to the vertical middle plane of the tires. Braking forces, which act along the lines of intersection of the vertical middle planes of the tires and the road surface, are denoted as F_{xi}. The linear restoring moment about the king pin axis (produced by the stabilizing system attached to the wheels) is given by $KS \rightarrow K\delta$, wherein K is the effective spring constant.

P_1 and P_2 locate the center of mass for the left and right wheel assemblies, respectively. The complete derivation of the accelerations, $\bar{a}_{p1}$ and $\bar{a}_{p2}$, is shown in Appendix B. An abbreviated derivation for $\bar{a}_{p2}$ is presented here to provide continuity. Chasle's Theorem for relative motion is

$$\bar{a}_{p2} = \bar{a}_0 + \bar{a}_{p2/0}.$$

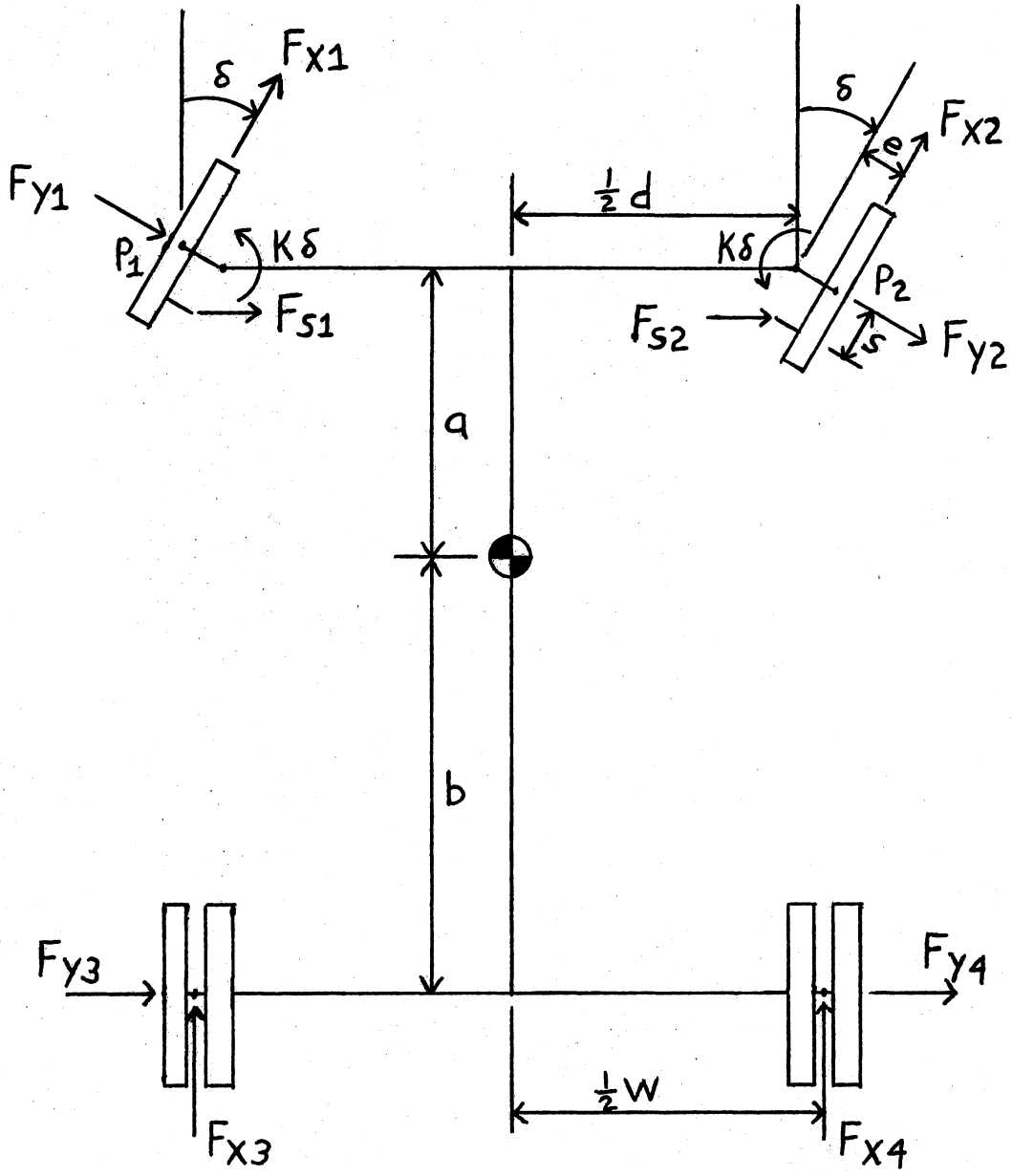

Figure 3. Diagram of the Forces Which Act on the Vehicle

Furthermore,

$$\bar{R}_p = \bar{R}_0 + \bar{\rho}_1 + \bar{\rho}_2.$$

The validity of the two equations is evident from Figures 1 and 3 where

$$\bar{\rho}_1 = ai + \frac{1}{2} dj$$

and

$$\bar{\rho}_2 = (-e \sin \delta)i + (e \cos \delta)j.$$

Differentiation of $\bar{R}_p$ yields

$$\dot{\bar{R}}_p = \dot{\bar{R}}_0 + \dot{\theta}(-\frac{1}{2} di + aj) + e(\dot{\delta} + \dot{\theta})[\cos\delta i + \sin\delta j].$$

Taking the derivative of $\dot{\bar{R}}_p$ and making the substitution $\beta = \theta + \delta$ produces

$$\bar{a}_{p2} = [e \dot{\beta}^2 \sin\delta - e \ddot{\beta} \cos\delta - \frac{1}{2} d \ddot{\theta} - a \dot{\theta}^2 + \dot{U} - V \cdot r]i$$

$$- [e \dot{\beta}^2 \cos\delta + e \ddot{\beta} \sin\delta + \frac{1}{2} d \dot{\theta}^2 - a \ddot{\theta} - \dot{V} - U \cdot r]j, \quad (4)$$

and

$$\bar{a}_{p1} = [-e \dot{\beta}^2 \sin\delta + e \ddot{\beta} \cos\delta + \frac{1}{2} d \ddot{\theta} - a \dot{\theta}^2 + \dot{U} - V \cdot r]i$$

$$+ [e \dot{\beta}^2 \cos\delta + e \ddot{\beta} \sin\delta + \frac{1}{2} d \dot{\theta}^2 + a \ddot{\theta} + \dot{V} + U \cdot r]j. \quad (5)$$

Figures 4 and 5 show the forces applied to the left and right wheels, respectively, and Figure 6 shows those associated with the vehicle body. Applying Newton's Laws to the left wheel results in

$$m_{w1} a_{p1y} = R_{y1} + F_{s1} + F_{y1} \cos\delta + F_{x1} \sin\delta, \quad (6)$$

$$m_{w1} a_{p1x} = R_{x1} - F_{y1} \sin\delta + F_{x1} \cos\delta, \quad (7)$$

$$I_{w1} \ddot{\beta}_1 = -K\delta - F_{s1} (s \cos\delta + e \sin\delta) - R_{y1} e \sin\delta$$

$$- R_{x1} e \cos\delta, \quad (8)$$

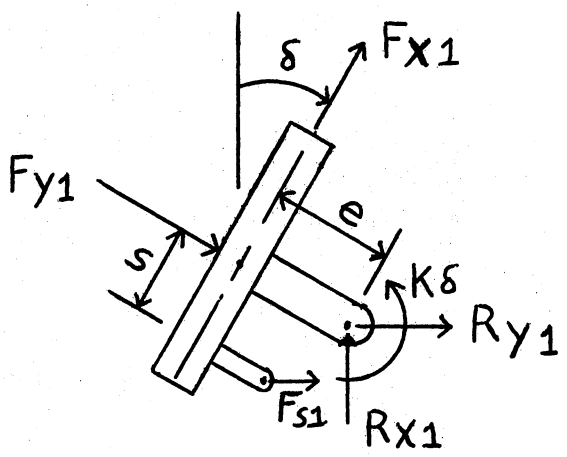

Figure 4. Forces Which Act on the Left Front Wheel

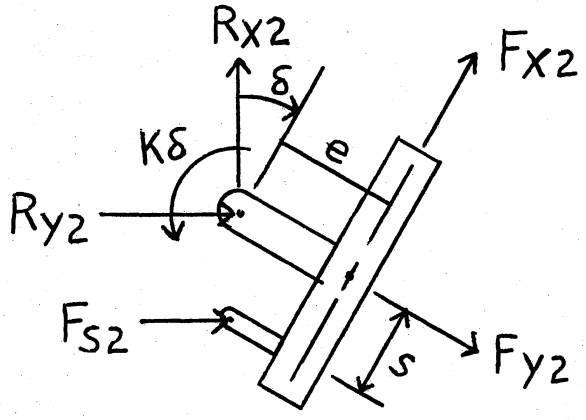

Figure 5. Forces Which Act on the Right Front Wheel

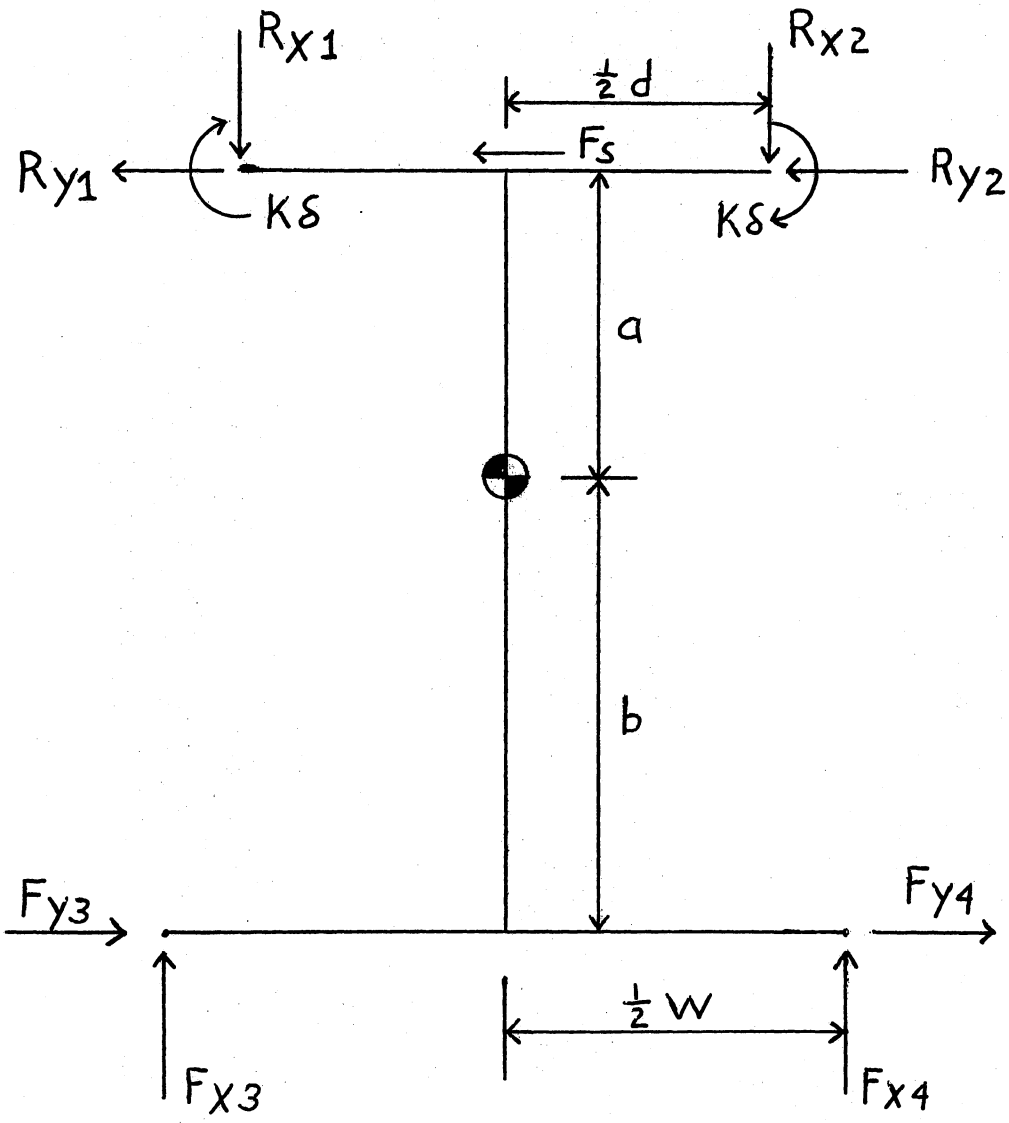

Figure 6. Free-Body Diagram for the Vehicle (Less the Front Wheels)

wherein $\ddot{\beta} \equiv \ddot{\theta} + \ddot{\delta}$ is the angular acceleration of the left front wheel. For the right wheel Newton's Laws yield

$$m_{w2}\, a_{p2y} = R_{y2} + F_{s2} + F_{x2} \sin\delta + F_{y2} \cos\delta, \tag{9}$$

$$m_{w2}\, a_{p2x} = R_{x2} + F_{x2} \cos\delta - F_{y2} \sin\delta, \tag{10}$$

$$I_{w2}\, \ddot{\beta}_2 = -K\delta - F_{s2} [s \cos\delta - e \sin\delta] + R_{x2}\, e \cos\delta + R_{y2}\, e \sin\delta, \tag{11}$$

because of the constraint provided by the tie-rod, $\beta_1 = \beta_2$. By combining Equations (6) to (11), a single expression for $\ddot{\beta}$ is obtained (Appendix C). From Equation (C-10),

$$\ddot{\beta} = \frac{1}{I_w + m_w e^2} \left[-K\delta - \frac{1}{2} F_s\, S \cos\delta + \frac{1}{2} e\, (F_{x1} - F_{x2}) - \frac{1}{2} m_w\, e\, t\, (\dot{r} \cos\delta + r^2 \sin\delta)\right] \tag{12}$$

By applying Newton's Laws to the vehicle free-body shown in Figure 6, the equations of motion are obtained for the vehicle referred to body-centered axes through the center of gravity. The acceleration components have been derived previously and appear as the left sides of Equations (1), (2) and (3). Summing the forces in the x and y directions and the moments about the center of gravity (point 0) yields

$$m_c\, (\dot{U} - V \cdot r) = -R_{x1} - R_{x2} + F_{x3} + F_{x4} \tag{13}$$

$$m_c\, (\dot{V} + U \cdot r) = -R_{y1} - R_{y2} + F_{y3} + F_{y4} \tag{14}$$

$$I \cdot \dot{r} = -R_{y1} a - R_{y2} a - \frac{1}{2} d\, R_{x1} + \frac{1}{2} d\, R_{x2} - F_{y3} b + \frac{1}{2} w\, F_{x3} - b\, F_{y4} - \frac{1}{2} w\, F_{x4} + 2\, K\delta - a\, F_s \tag{15}$$

The reaction forces are eliminated using the expressions for R_{x1}, R_{x2}, R_{y1}, and R_{y2} from Equations (6), (7), (9), and (10). Substituting the acceleration components from Equations (4) and (5), and using $m_{w1} = m_{w2} = m_w$ and $\ddot{\theta} = \dot{r}$ yields

$$m_c (\dot{U} - V \cdot r) = -2 m_w (\dot{V} + U \cdot r) - 2 m_w a r + F_s + (F_{x1} + F_{x2}) \cos\delta + F_{x3} + F_{x4}$$

$$m_c (\dot{V} + U \cdot r) = -2 m_w (\dot{V} + U \cdot r) - 2 m_w a \dot{r} + F_s + (F_{x1} + F_{x2}) \sin\delta + (F_{y1} + F_{y2}) \cos\delta + F_{y3} + F_{y4}$$

$$I \cdot \dot{r} = -2 a m_w (\dot{V} + U \cdot r + a \dot{r}) + d m_w (e \dot{\beta}^2 \sin\delta - e \ddot{\beta} \cos\delta - \tfrac{1}{2} d \dot{r}) + F_{x1} (a \sin\delta + \tfrac{1}{2} d \cos\delta) + F_{y1} (a \cos\delta - \tfrac{1}{2} d \sin\delta) + F_{x2} (a \sin\delta - \tfrac{1}{2} \cos\delta) + F_{y2} (a \cos\delta + \tfrac{1}{2} \sin\delta) - b F_{y3} + \tfrac{1}{2} d F_{x3} - F_{y4} b - \tfrac{1}{2} d F_{x4} + 2 K\delta.$$

The equations of motion are now complete and describe the movement of the vehicle in terms of the four degrees-of-freedoms x, y, θ, and δ and their derivatives. These equations, when written in first-order form, appear as a set of nonlinear differential equations.

$$\dot{\gamma} = \frac{1}{I_w + m_w e^2} [-K\delta - \tfrac{1}{2} F_s S \cos\delta + \tfrac{1}{2} e (F_{x1} - F_{x2}) - \tfrac{1}{2} m_w e d (\dot{r} \cos\delta + r^2 \sin\delta)] \tag{16}$$

$$\dot{r} = \frac{1}{I_c + 2a^2 m_w + \frac{1}{2} d^2 m_w} [-2 a m_c (\dot{V} + U \cdot r)$$

$$+ m_c\, d\, e\, (\gamma^2 \sin\delta - \dot{\gamma}\cos\delta) + F_{x1}\,(a\sin\delta + \tfrac{1}{2} d\cos\delta)$$

$$+ F_{y1}\,(a\cos\delta - \tfrac{1}{2} d\sin\delta) + F_{x2}\,(a\sin\delta - \tfrac{1}{2} d\cos\delta)$$

$$+ F_{y2}\,(a\cos\delta + \tfrac{1}{2} d\sin\delta) - F_{y3}\, b + \tfrac{1}{2} w\, F_{x3} - b\, F_{y4}$$

$$- \tfrac{1}{2} w\, F_{x4} + 2\, K\delta]. \qquad (17)$$

$$\dot{U} = V\cdot r - \frac{2\, m_w}{m_c + 2\, m_w} a\, r^2 + \frac{1}{m_c + 2\, m_w}[(F_{x1} + F_{x2})\cos\delta$$

$$- (F_{y1} + F_{y2})\sin\delta + F_{x3} + F_{x4}. \qquad (18)$$

$$\dot{V} = -U\cdot r - \frac{2a\, m_w}{m_c + 2\, m_w}\dot{r} + \frac{1}{m_c + 2\, m_w}[(F_{y1} + F_{y2})\cos\delta$$

$$+ (F_{x1} + F_{x2})\sin\delta + F_{y3} + F_{y4}. \qquad (19)$$

$$\dot{\beta} = \gamma \qquad (20)$$

$$\dot{\theta} = r \qquad (21)$$

$$\dot{\delta} = \gamma - r \qquad (22)$$

$$\dot{R}_x = U + r\, R_y \qquad (23)$$

$$\dot{R}_y = V - r\, R_x \qquad (24)$$

The tire side-forces (F_{yi}) appear in Equations (17), (18) and (19). The side-force is a function of the normal force (vertical load on the tire) and the tire slip-angle (angle between the wheel heading and the direction of the velocity vector for the point of contact).

Equations for Normal Forces Acting on the Tires

Due to the vehicle inertia, the vertical load at each axle has a dynamic term in addition to the static load. Figure 7 illustrates the

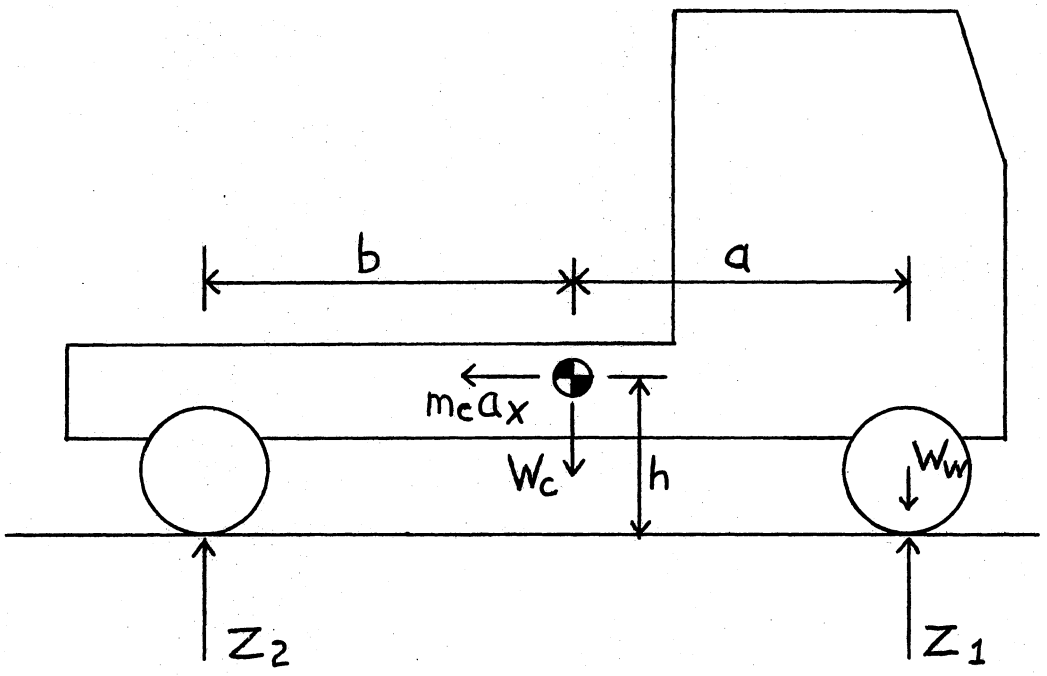

Figure 7. Normal Forces and Weight Transfer During Forward Acceleration

forces associated with the acceleration in the forward direction. Applying Newton's Laws, the resulting expressions for the front and rear vertical loads, Z_1 and Z_2 respectively, are

$$Z_1 = m_c\, g - \frac{m_c\, a\, g}{a + b} - \frac{m_c\, (U - V \cdot r)\, h}{a + b};$$

$$Z_2 = \frac{m_c\, g\, a}{a + b} + \frac{m_c\, (U - V \cdot r)\, h}{a + b}.$$

The forces on the front axle are shown in Figure 8 where

$$m_f = m_c - \frac{m_c\, a}{a + b} - \frac{m_c\, h\, (\dot{U} - V \cdot r)}{g\, (a + b)};$$

$$f = \frac{1}{2}\, d + e.$$

Application of Newton's Laws yield

$$F_{z1} = m_w\, g + \frac{1}{2}\, m_c\, g - \frac{1}{2}\, \frac{m_c\, g\, a}{a + b} - \frac{1}{2}\, \frac{m_c\, h}{g\, (a + b)}\, (\dot{U} - V \cdot r) + \left(\frac{m_c\, h}{f} - \frac{m_c\, h\, g}{f\, (a + b)}\right) \dot{V} + U \cdot r - \frac{m_c\, h^2}{f\, g\, (a + b)}\, (\dot{U} - V \cdot r)\, (\dot{V} + U \cdot r). \tag{25}$$

$$F_{z2} = m_w\, g + \frac{1}{2}\, g\, m_w - \frac{1}{2}\, \frac{m_c\, g\, a}{a + b} - \frac{1}{2}\, \frac{m_c\, h}{g\, (a + b)}\, (\dot{U} - V \cdot r) + \left(\frac{m_c\, a\, h}{f\, (a + b)} - \frac{m_c\, h}{f}\right)(\dot{V} + U \cdot r) + \frac{m_c\, h^2}{f\, g\, (a + b)}\, (\dot{U} - V \cdot r)\, (\dot{V} + U \cdot r). \tag{26}$$

The rear axle forces are shown in Figure 9 where

$$m_r = m_c - \frac{m\, a}{(a + b)} - \frac{m_c\, h\, (\dot{U} - V \cdot r)}{g\, (a + b)}.$$

Normal forces resulting from Newton's Laws are

$$F_{z3} = \frac{1}{2}\, \frac{m_c\, g\, a}{(a + b)} + \frac{1}{2}\, \frac{m_c\, h\, (\dot{U} - V \cdot r)}{(a + b)}$$

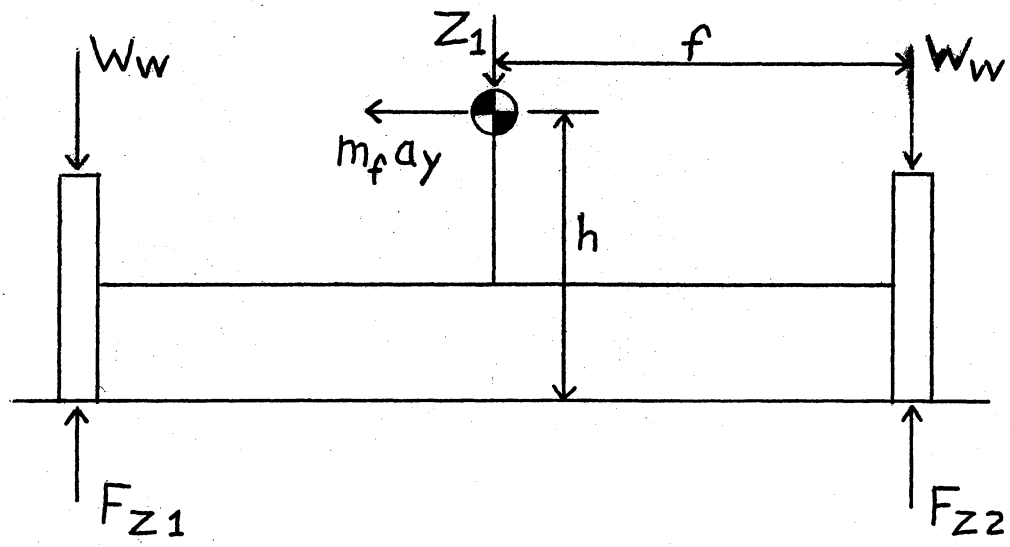

Figure 8. Free-Body Diagram Used to Calculate Front Wheel Normal Forces

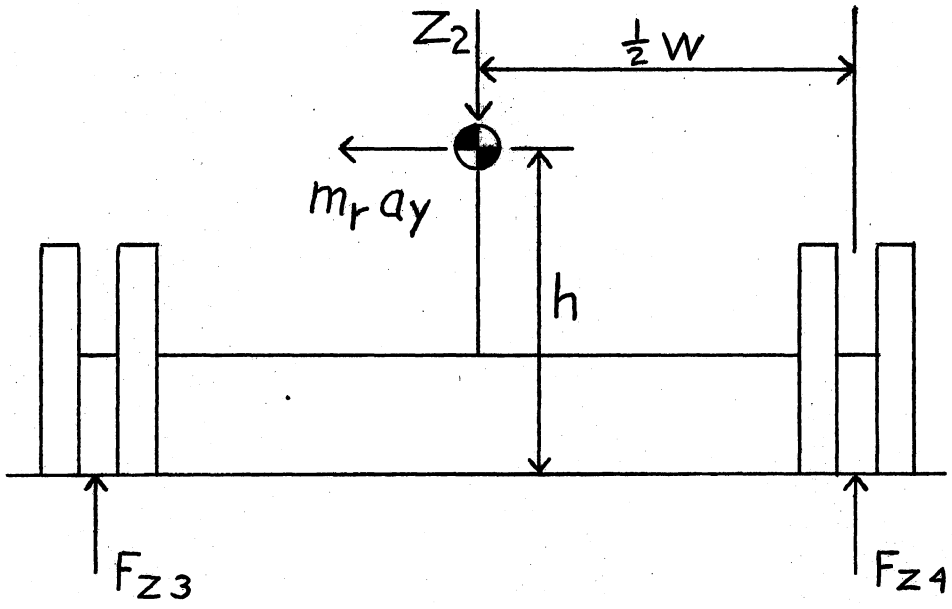

Figure 9. Free-Body Diagram Used to Calculate Rear Wheel Normal Forces

$$+ \frac{m_c\, h\, (\dot{V} + U \cdot r)}{w\, (a + b)} \left[a + \frac{h\, (\dot{U} - V \cdot r)}{g}\right]. \tag{27}$$

$$F_{z4} = \frac{1}{2} \frac{m_c\, g\, a}{(a + b)} + \frac{1}{2} \frac{m_c\, h\, (\dot{U} - V \cdot r)}{(a + b)}$$

$$- \frac{m_c\, h\, (\dot{V} + U \cdot r)}{w\, (a + b)} \left[a + \frac{h\, (\dot{U} - V \cdot r)}{g}\right]. \tag{28}$$

Front Slip Angle Equations

The derivation of an expression for the front slip angle utilizes both the velocity vector of the point of road contact of the front tire and a vector in the direction of the front wheel heading. For simplicity, the point of road contact is assumed to lie on a vertical line passing through the center of mass of the front wheel assembly. Therefore, and also because the motion is constrained to a horizontal plane, the velocity of each point of road contact is equivalent to the velocity of the center of mass of each wheel assembly. The acceleration of the contact point may be denoted as $\bar{a}_{po}$. From the derivation of $\bar{a}_{po}$ (Appendix B), $\dot{\bar{R}}_p$ can be expressed as

$$\dot{\bar{R}}_p = (\dot{R}_x - r R_y - \frac{1}{2} d r - e \dot{\beta} \cos\delta) i + (\dot{R}_y + r R_x + a r$$

$$- e \dot{\beta} \sin\delta) j;$$

$$\dot{\bar{R}}_p = R_{px} i + R_{py} j.$$

The wheel heading angle ψ is expressible as

$$\psi = \frac{1}{2} \pi - \delta.$$

The angle (ϕ) of the velocity-vector is obtained by using the relation

$$\phi = \text{Arc tan } (R_{px}/R_{py}).$$

Therefore, the front slip angle is $\psi - \phi$. These expressions are valid if $\delta > 0$ and $R_{py} > 0$. Similar expressions are used for the case when $\delta \leq 0$ and $R_{py} \leq 0$.

$$\psi = \frac{1}{2}\pi - \delta$$

$$\phi = \frac{1}{2}\pi + \text{Arc tan } (-R_{py}/R_{px})$$

$$\alpha_f = \psi - \phi.$$

Rear Slip Angle Equations

Although the rear slip angle (α_r) can be obtained by a previous method, a different procedure is used because the rear wheel heading is always in the direction of the unit vector i. Appendix D contains the complete derivation of α_r. By defining q as the point of contact for the rear tires, the velocity vector is given as

$$\dot{\bar{R}}_q = (\dot{R}_x - r R_y - \frac{1}{2} w r)i + (\dot{R}_y + r R_x - b r)j$$

or

$$\dot{\bar{R}}_q = R_{qx}i + R_{qy}j.$$

Using the definition of the dot product

$$\bar{A} \cdot \bar{B} = |AB| \cos\alpha,$$

the rear slip angle can be expressed in terms of $\dot{\bar{R}}_q$ and the unit vector i.

$$\dot{\bar{R}}_q \cdot i = |\dot{\bar{R}}_q| \cos\alpha_r.$$

Therefore,

$$\alpha_r = \text{Arc cos } \left(\frac{R_{qx}}{\sqrt{R_{qx}^2 + R_{qy}^2}}\right). \tag{29}$$

The sign of α_r is the same as the sign of R_{qy}. Knowing the normal forces and slip angles, the tire side-forces can be read from Figure 10 showing F_y (empirically) as a function of F_z and α.

Transfer Equations for the Axis Systems

Equations (16) through (24) are derived with reference to the moving axis system x-y. It is useful, however, to express the position of the center of gravity referred to the fixed axis system X-Y. From Figure 1 the transfer equations can be seen to be expressible as

$$R_X = -R_y \sin\theta + R_x \cos\theta \tag{30}$$

and

$$R_Y = R_y \cos\theta + R_x \sin\theta. \tag{31}$$

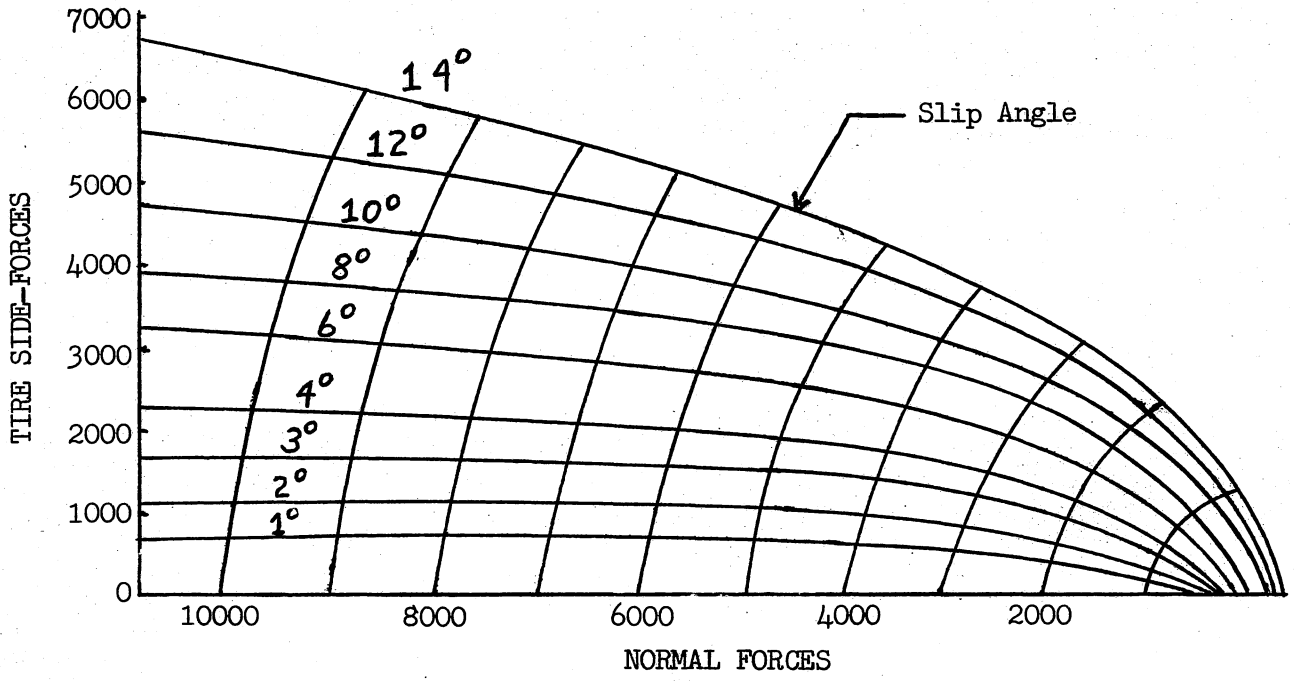

Figure 10. Graph of Tire Side-Forces Versus Normal Forces and Slip Angles

CHAPTER III

COMPUTER SOLUTION

As shown in the previous chapter, the motion of the vehicle can be described by a set of nine first-order, nonlinear differential equations. The solution to this set of equations was obtained using the Oklahoma State University IBM 360/65 digital computer and "DYSIMP" (a continuous DYnamic SIMulation Program). DYSIMP was developed by students and faculty from the School of Mechanical and Aerospace Engineering and has the capability of solving, simultaneously, a maximum of 100 first-order differential equations. Integration methods available to the user are the (1) simple Euler, (2) modified Euler, and (3) fourth-order Runge-Kutta methods. The standard program output consists of up-to-five tables, each containing time-histories of up-to-ten variables. Five printer-plots, each containing as many as five variables, can also be produced. The program is coded in FORTRAN IV and may be executed in either single or double precision.

The differential equations to be solved for this research problem were supplied to DYSIMP using a "derivative subroutine." Therefore, programming the solution involved developing a sequence of computer operations to evaluate the nine derivatives appearing in the set of nine differential equations.

Evaluation of the derivatives depended upon the state variables, steering force (F_s), braking forces (F_{xi}), and tire side-forces (F_{yi}).

F_s is a linear function of the state variables and F_{xi} is prescribed by the user as a function of time. However, F_{yi} is a nonlinear, empirically determined function of the slip-angle and normal forces (F_{zi}) which are, in turn, dependent on $\dot{U}$ and $\dot{V}$. A "look-up table" subroutine was used to find F_{yi} and this prevented the development of expressions for $\dot{U}$ and $\dot{V}$ which would involve F_{yi} directly. By choosing the integration step-size sufficiently small, calculation of the normal forces could be made using values for the derivatives from the previous time-step. (Between any two time steps, the greatest change in F_{yi} was found to be less than five percent of its maximum value.)

As stated earlier, the tire side-forces were obtained using a "look-up table" subroutine. In previous studies, investigators calculated F_{yi} using empirical equations to approximate test data. Figure 10 shows a plot of the side-force (F_{yi}) versus normal force (F_{zi}) and slip-angle for a specific truck tire. A two-dimensional table was set up using F_{yi} as a tabulated function of the F_{zi} and the slip-angle. Even-increments were used on both axes (normal force and slip angle) and a three-step, linear interpolation procedure was used for the intermediate values.

After the tire side-forces were evaluated, the derivatives for one time-step were expressed in terms of known quantities. Although the set of equations is linear in the time-domain, the $\dot{\gamma}$, $\dot{r}$, and $\dot{v}$ equations are coupled by the derivative terms. A subroutine called "SIMQ" was used to solve for these three derivative values. The other six derivative expressions were direct evaluations. With these values, the derivative subroutine was then input to the main program and the integration was

performed for one time-increment using the Runge-Kutta fourth-order method. DYSIMP called the subroutine for each time-step.

A brief flow-chart describing the sequence of operations for the derivative subroutine is shown by Figure 11. The look-up table algorithm was also supplied to DYSIMP in the derivative subroutine with the addition of one control card.

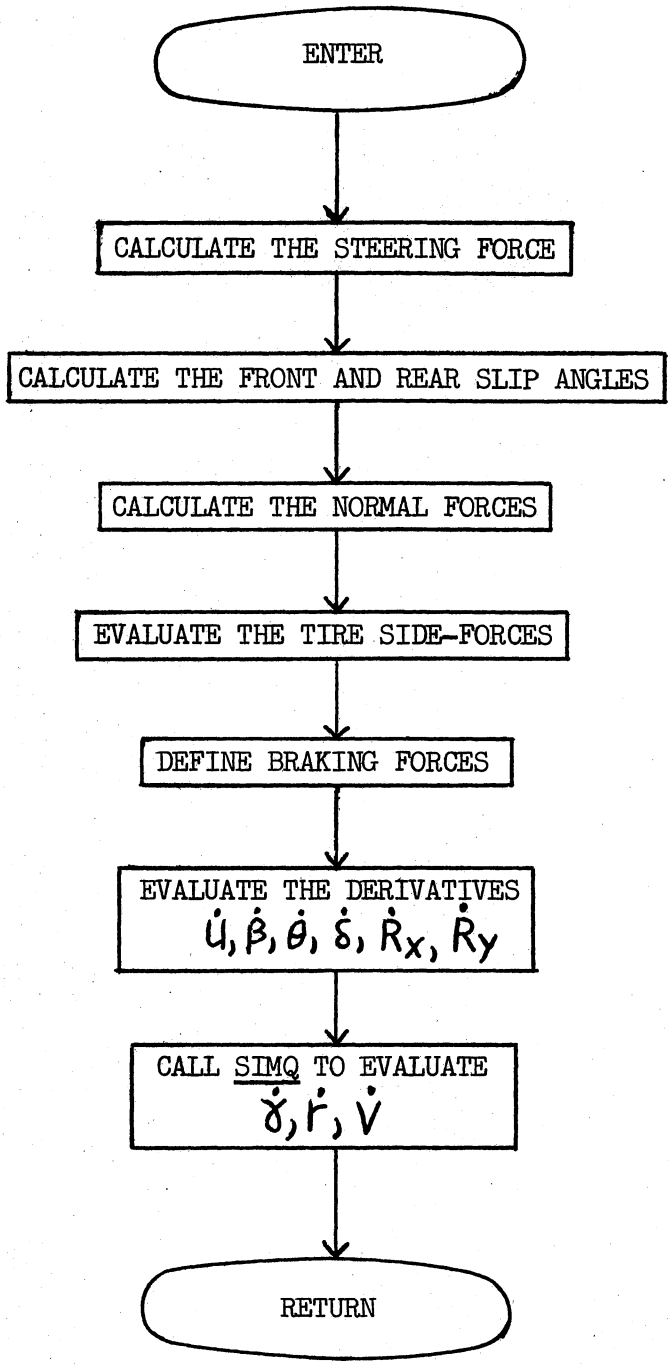

Figure 11. Flow Diagram of Derivative Subroutine

CHAPTER IV

NUMERICAL RESULTS

Verification of the Program

After the program was written and "de-bugged," a study of several simple cases was made to verify that the computed results were accurate (qualitatively, at least) and reasonable. Although these cases were relatively simple, no shortcuts in the computation sequence were made, thus verifying that the entire program was functioning properly.

Using a sample problem, a search was made to determine the typical step-size needed for numerical stability. The integration was performed over a maximum time-period of twenty seconds. Applying a step-function steering force of 31 pounds, beginning at three seconds, and using K=50 ft-lb/rad, solutions were found for computing increments of .500, .250, .125, and .100 seconds. Figure 12 illustrates the computed response of $\dot{V}$ for three of the step-sizes. (The results using a time-increment of .500 seconds were highly unstable and are not shown on Figure 12.) It was concluded that .125 seconds was an acceptable step-size and was used in all the remaining computer solutions. This appeared to be satisfactory for maintaining numerical stability.

Three alternating-direction forces were applied during a twenty-second period to the steering arm to observe the quality of the physical response. Because of the sign convention, a positive force should

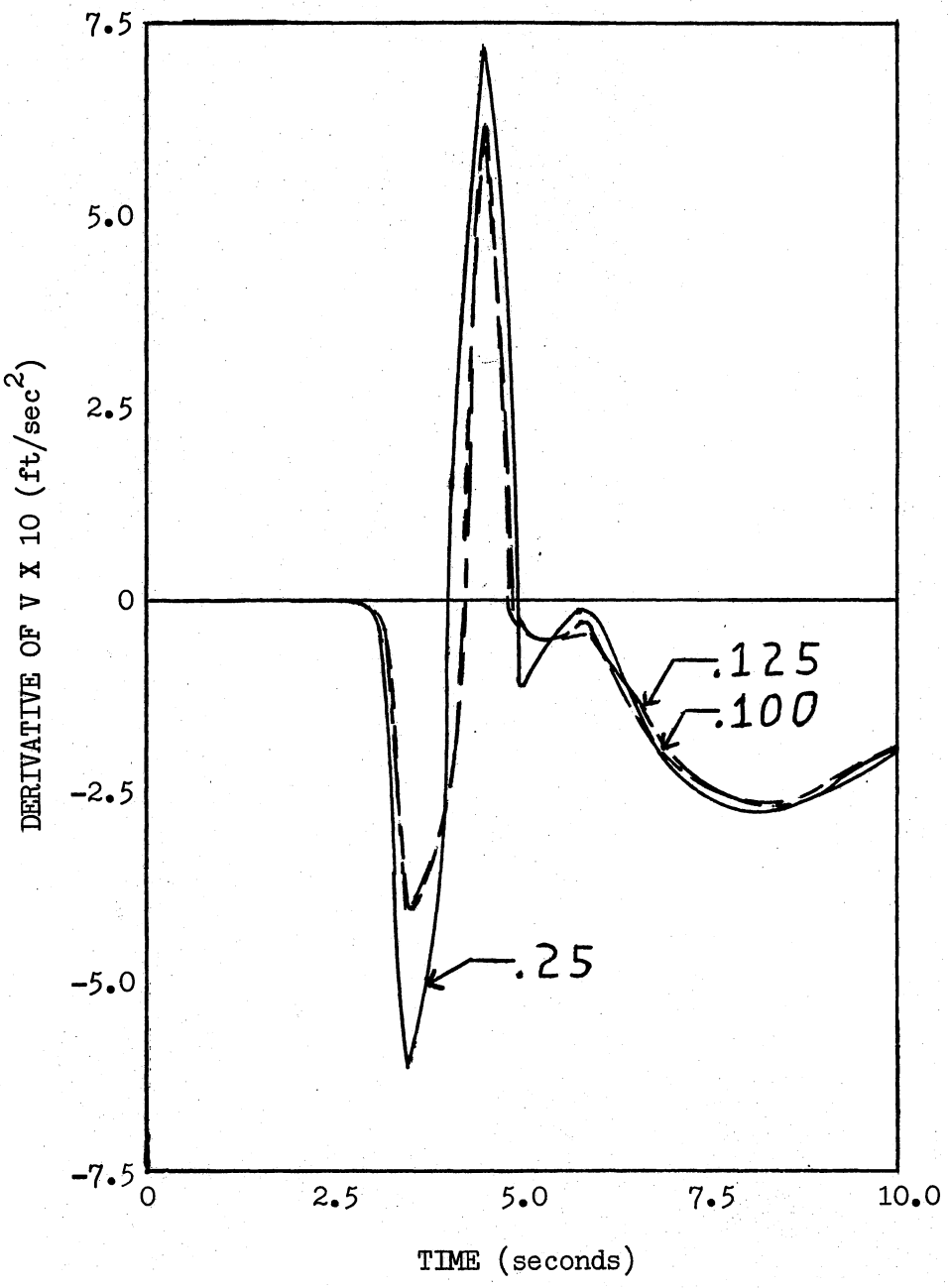

Figure 12. The Response of $\dot{V}$ for Δt Step-Sizes of .250, .125, and .100

create a negative wheel-angle. The three applied forces and corresponding points of application were: (1) +20 lbf @ 80 ft, (2) -40 lbf @ 220 ft, and (3) +40 lbf @ 560 ft. (F_s acting to the left is taken to be positive.) These forces were applied for a duration of one second and the input force was held at zero for all other times. The initial value of the forward velocity (U) was 40 ft/sec while all other variables were initially zero.

The varying wheel angles resulting from applying these forces are shown in Figure 13 for two different spring stabilizer constants (K=0 and K=100). For this same study the path of travel for the vehicle center of gravity (C.G.) is shown by Figure 14. Although there have been no previous studies with which to compare these results, they seem to be reasonable.

Another study was made to check the simulation by applying both equal and unequal braking forces at the rear wheels. The vehicle was given an initial forward velocity of 40 ft/sec and all other variables initialized as zero. A braking force of -400. lbf (forward forces are taken to be positive) was applied at t=3 seconds to each of the rear wheels. Figure 15 shows the path of travel to be unaltered, as expected. It should also be noted that the angular rotation of the vehicle remained zero (as it should) during the entire braking period.

From the equation of motion (F=ma), the acceleration can be determined for the case of equal braking forces. The forces are constant and, therefore, the acceleration is constant. For constant acceleration along a linear path, the velocity may be found at any point using the expression $V^2 = V_o^2 + 2a\,(S-S_o)$. This expression matches very well with the numerical solution as can be seen from Figure 16.

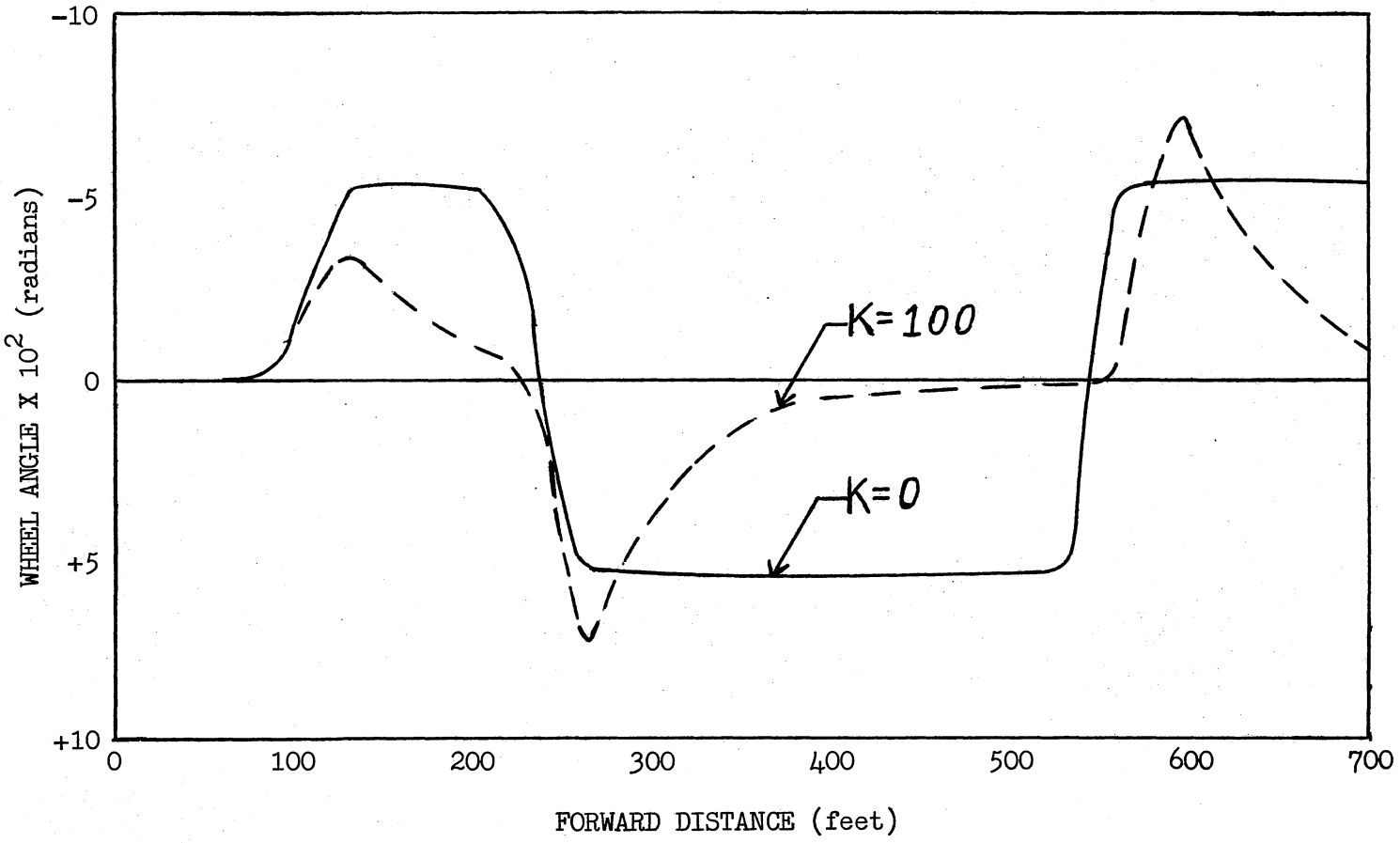

Figure 13. Wheel Angle Resulting From an Impulse Steering Force

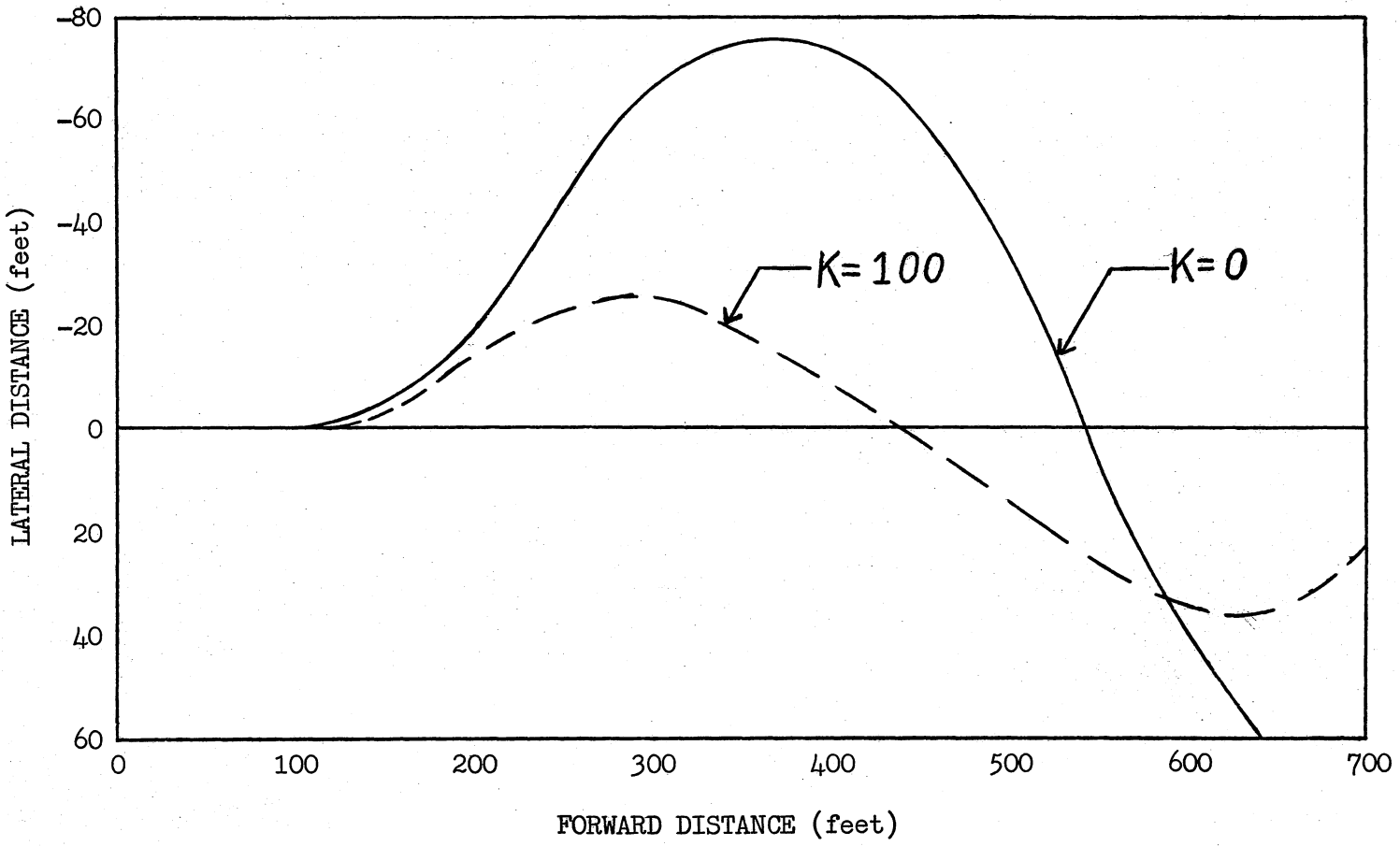

Figure 14. The Path of Travel of the Vehicle C.G. Resulting From the Impulse Steering Force

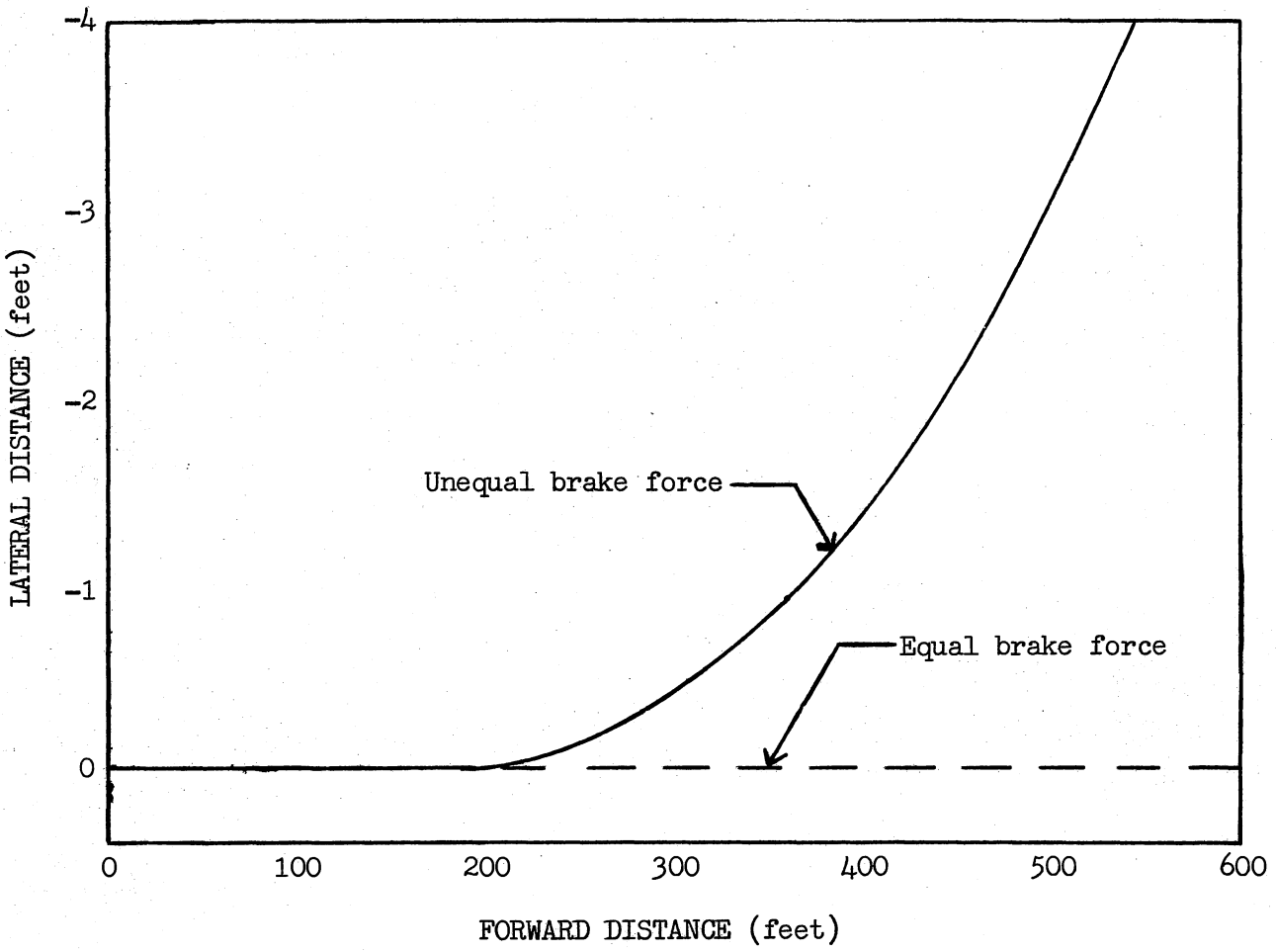

Figure 15. Travel of the Vehicle Center of Mass During Braking

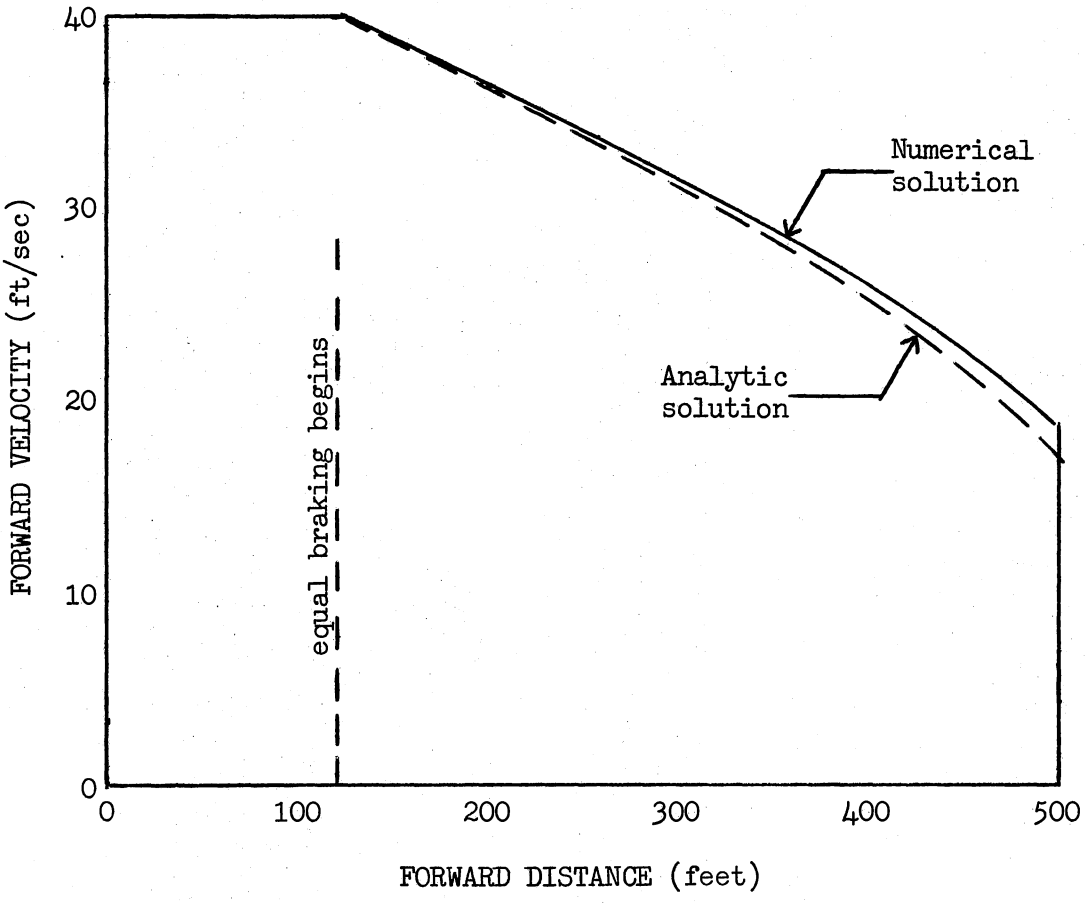

Figure 16. Comparison of the Numerical and Analytical Solution of Forward Velocity

The same initial conditions as before were used for the case of unequal braking forces. After three seconds, forces of -425. lbf and -300. lbf were applied to the left and right rear wheels, respectively. The path of travel for the vehicle C.G. for this situation may also be observed from Figure 15. Application of a larger left-wheel force pulls the vehicle to the left as it should.

Although these few cases hardly verified the applicability of the computer solution to all anticipated situations, the results of these studies were reassuring and were judged to be sufficient for a continuation into the next phase of the research. Certainly, the true test of applicability of this method would be correlation with results taken experimentally, but such verification is beyond the scope of this present research effort.

Analysis of Situations Which May Occur During Normal Driving

After having gained some confidence that the methodology and the computer program were reliable, a study was undertaken to gain quantitative insight into the characteristic behaviors of typical vehicles during simulated front-tire impacts and failures. Also, a major objective of this portion of the research was to gain some awareness of the effectiveness of simple mechanical spring-type steering stabilizer devices.

A study was made to determine the effect of the steering stabilizer device during an impact load applied to the left front wheel. A simplified simulation was made of the impulse forces resulting from the front wheel encountering a hole or bump in the road. For this case the

response characteristics studied were (1) the path of travel of the vehicle C.G. and (2) the steering arm force associated with that path.

In an attempt to simulate, approximately, the action taken by the driver, the restoring steering force was expressed as a linear function of the vehicle rotation and the wheel angle ($F_s = C_1\theta + C_2\delta$). Both constants were arbitrarily assigned a value of 600. The initial forward velocity was chosen to be 40 ft/sec and all other input variables taken to be initially zero. An impact force of -100 lbf was applied to the left front wheel over the time interval from 2.0 to 2.125 seconds. The driver reaction time was estimated to be about $1\frac{1}{8}$ seconds. Therefore, a steering force was not applied until 3.125 seconds (i.e., the vehicle had traveled forward approximately 45 feet).

Three different spring constants (0, 100 and 200 ft-lbs/rad) were used for this simulated front wheel disturbance. Figure 17 shows the different paths of travel for the C.G. The steering forces associated with the three spring-constant values are shown by Figure 18. Although the difference in the lateral movement of the C.G. between K=0 (effectively no spring stabilizer) and K=200 is only approximately 1.5 ft, this small distance could be sufficient to keep the driver from entering the lane of oncoming traffic and, thus, is enough to prevent an accident. Steering forces for this study were small, but it should be noted that K=0 yielded forces which were over twice those for K=200. For a relatively large spring constant, significantly less driver effort is experienced.

Tires blowing out on the front wheels may create forces which cause the driver to lose control of the vehicle. A study was made to determine if a spring stabilizer will increase the controlability of the vehicle

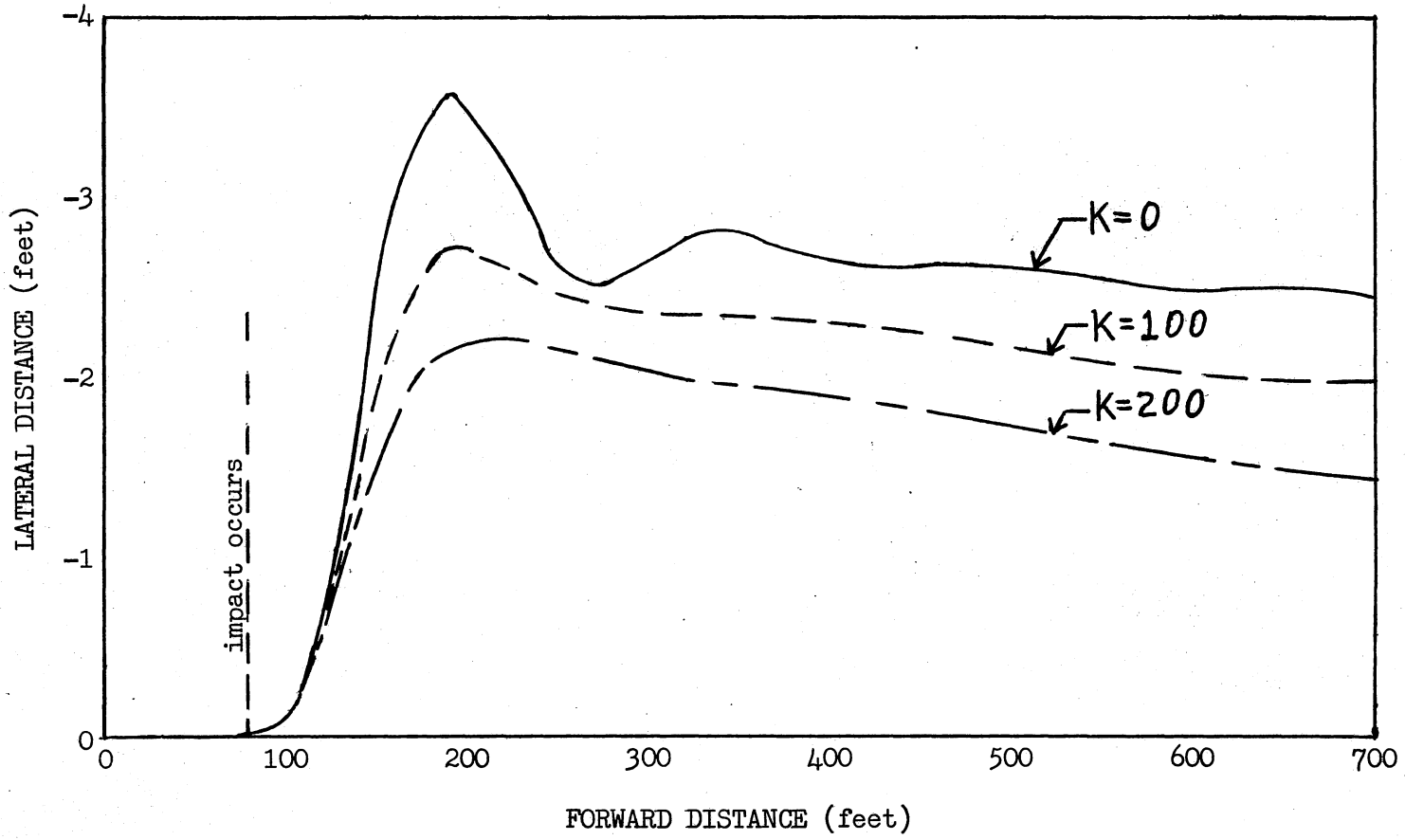

Figure 17. C.G. Response to Left-Wheel Impact

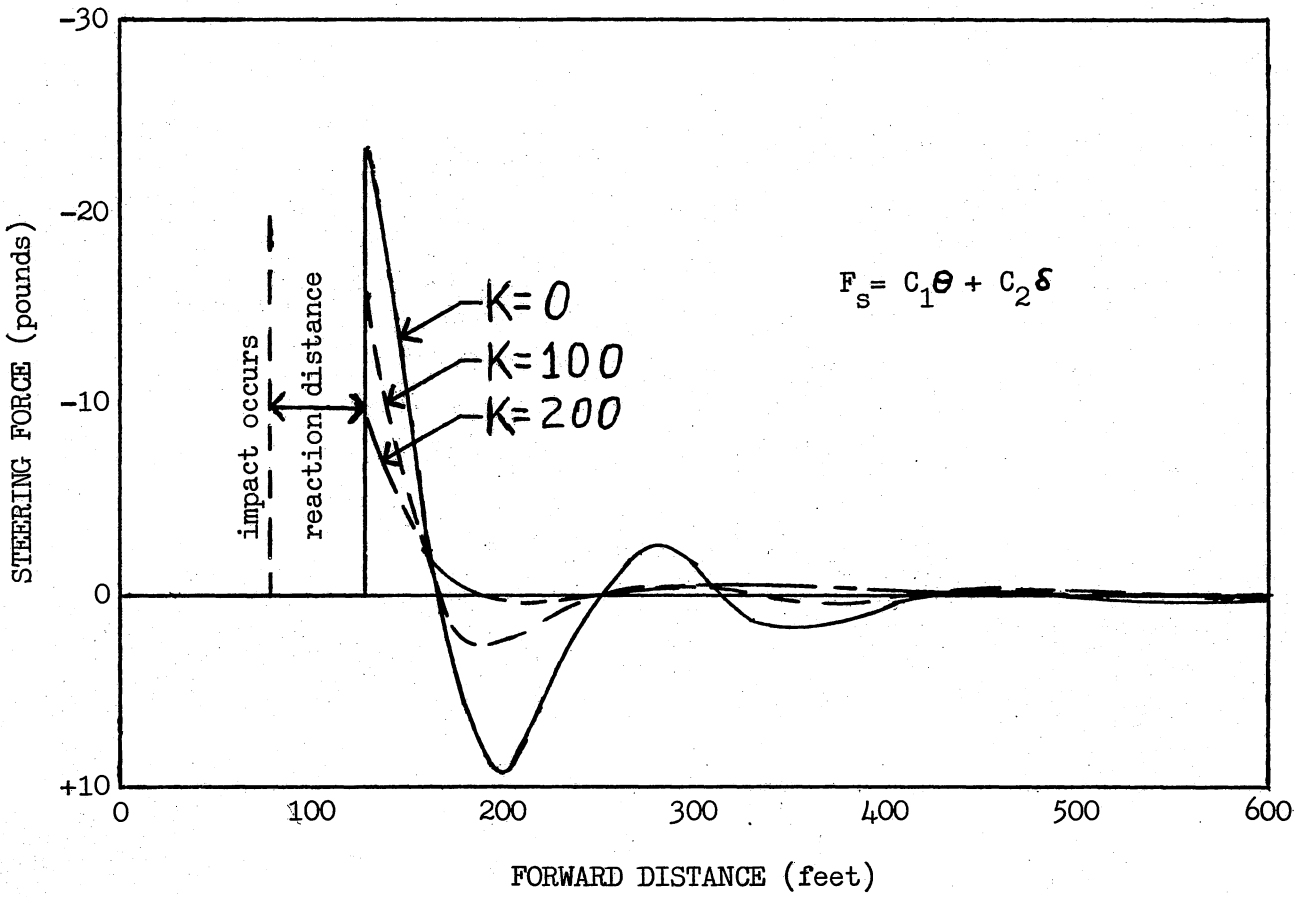

Figure 18. Steering Forces Corresponding to Left-Wheel Impact

during a blowout. The front-wheel forces during a blowout depend on tire size, vehicle speed, deflation time, and other factors. These factors are not easily determined. Therefore, for the present study an approximation was used. By applying kinematic principles and judgment, a forcing function, shown by Figure 19, was selected and applied, computationally, to the left front wheel.

The steering force for this study was expressed as $F_s = C_1\theta + C_2\delta + C_3$ where C_1 = 300 lbs/rad, C_2 = 600 lbs/rad, and C_3 = -26 lbs. The driver reaction time was, again, taken to be $1\frac{1}{8}$ seconds. Initial conditions chosen were U = 40 ft/sec and other variables taken initially to be zero.

Again, using three values of K (0, 100, 200), the three paths of the C.G. were computed and are shown by Figure 20. Steering forces associated with these paths are shown by Figure 21.

For this blowout simulation, the C.G. traveled slightly more than 23 ft to the left of the intended path without the spring stabilizer (i.e., for K=0). However, using K=200, the maximum distance to the left was 18.7 ft. The extra 4.3 ft could, perhaps, result in the vehicle entering an unsafe region or running off the left shoulder. The steady-state responses for all three cases are nearly identical. The simulated steering force contained no component to drive the vehicle back along the original path but, instead, was intended only to restore it to a path parallel to that of the main roadway. A maximum steering force of -125 lbf was needed using the "stiffer" (K=200) stabilizer while a force of -205 lbf was required with no stabilizer at all. Although these are merely representative numbers, the analysis showed that approximately

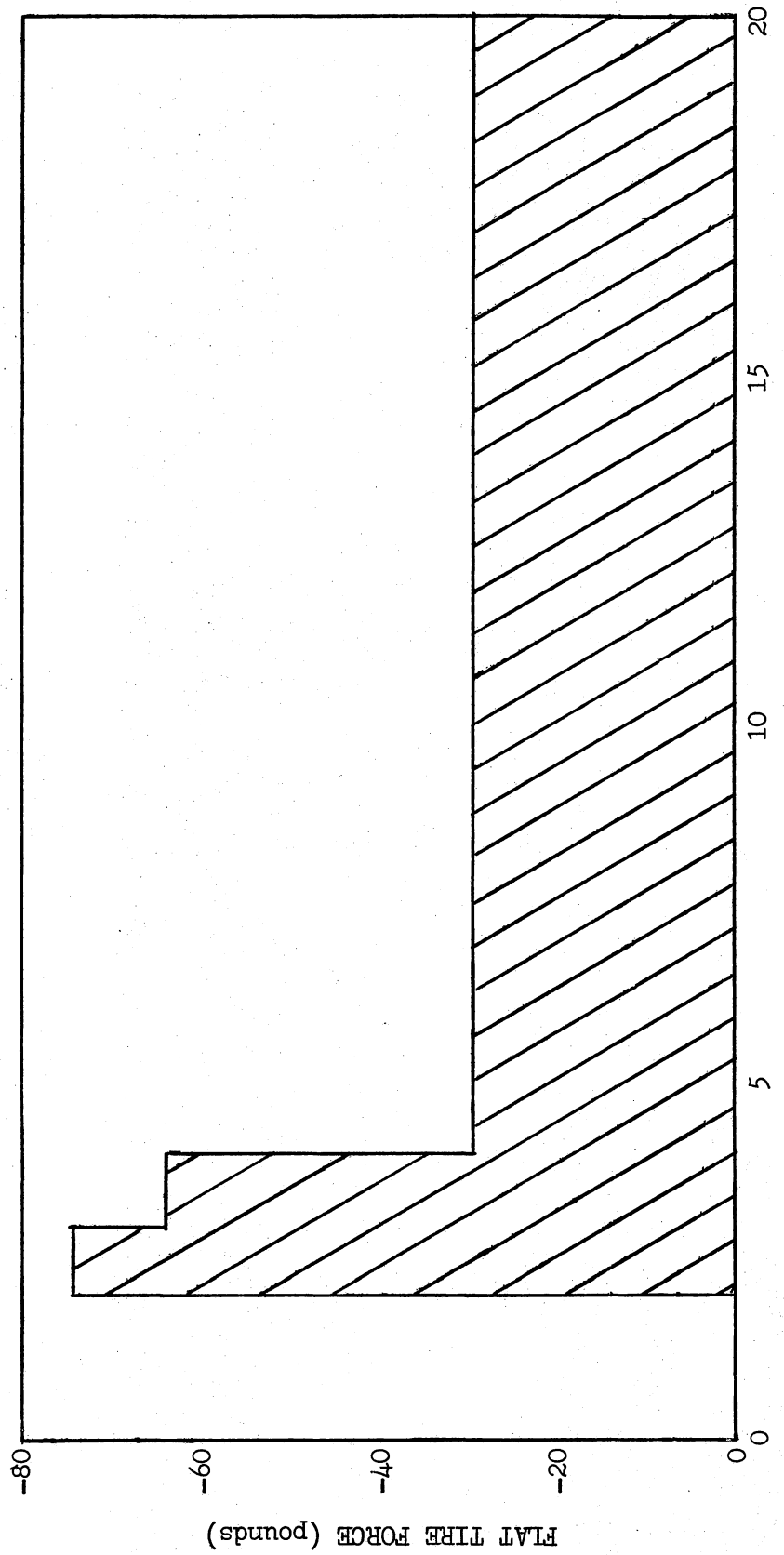

Figure 19. Force Simulation for a Blowout

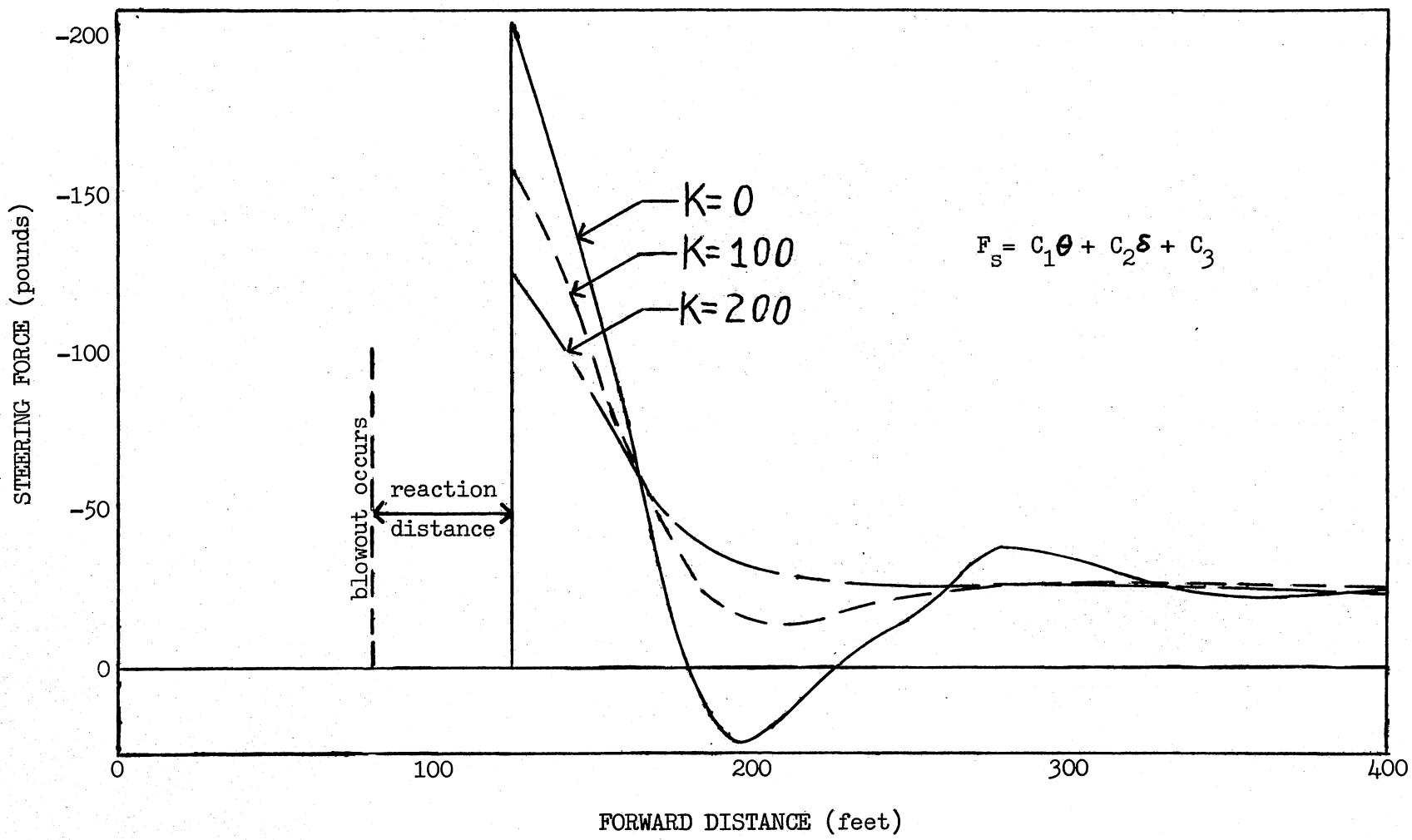

Figure 20. Path of the C.G. During a Blowout

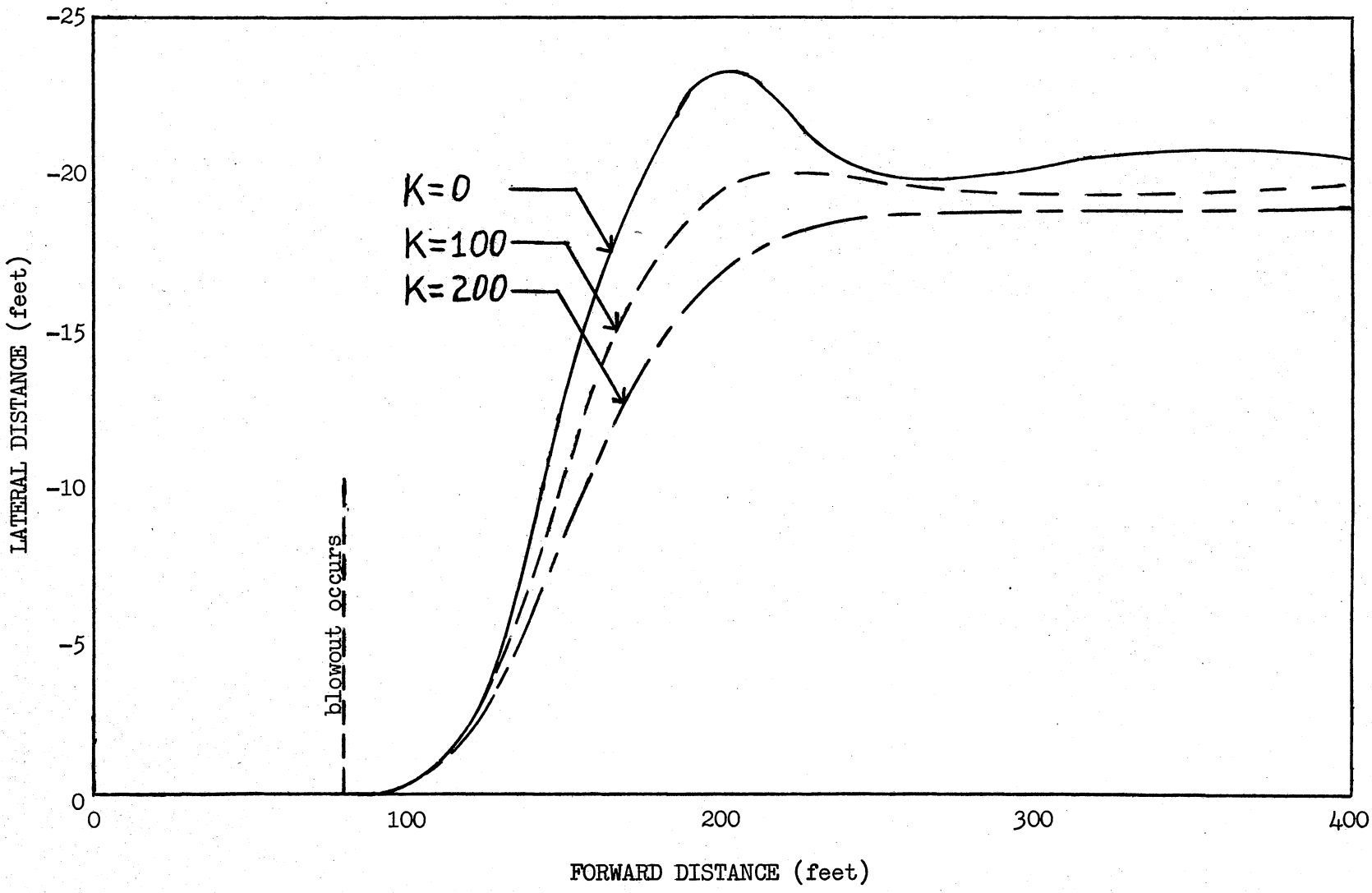

Figure 21. Steering Forces Associated With a Blowout

70 percent more force would be required if the vehicle were not equipped with a steering stabilizer.

A centering device tends to keep the vehicle in a straight line and may actually hinder the response when a change in heading (i.e., manueverability) is desired. The objective of the next study was to determine the effect of the stabilizer when a normal change in heading is made. The steering force used for this study was a linear function of the rotation angle (θ) and the velocity of rotation (r), (i.e., $F_s = C_1 (\theta+r)$ where $C_1 = 300$). The chosen initial conditions were U = 60 ft/sec and θ = 4 degrees. All other variables were initialized as zero. Constant and equal braking forces of -800 lbf were applied after .5 sec to each of the rear wheels. The chosen initial conditions and the selected braking forces may physically reflect a vehicle being pulled off the roadway onto the right shoulder as in a normal stopping maneuver. No steering force was applied until the vehicle C.G. had traveled 6 ft to the right. At this point the steering function was allowed to start "driving" the vehicle to change the heading angle from 4 degrees to 0 degrees.

The paths of travel for the C.G., using the three spring constants K = 0, 100, 200, are shown by Figure 22. Steering arm forces for all three cases were small and about the same magnitude. The maximum steering arm force was 16.0 lbf.

For the case of no stabilizer, the C.G. traveled 10.4 ft to the right and made the -4 degrees change in heading in only 106 ft of forward travel from the point of application of the steering force. However, for K = 200, the maximum distance to the right was 12.0 ft and the -4 degrees heading change required 400 ft of travel. A distance of

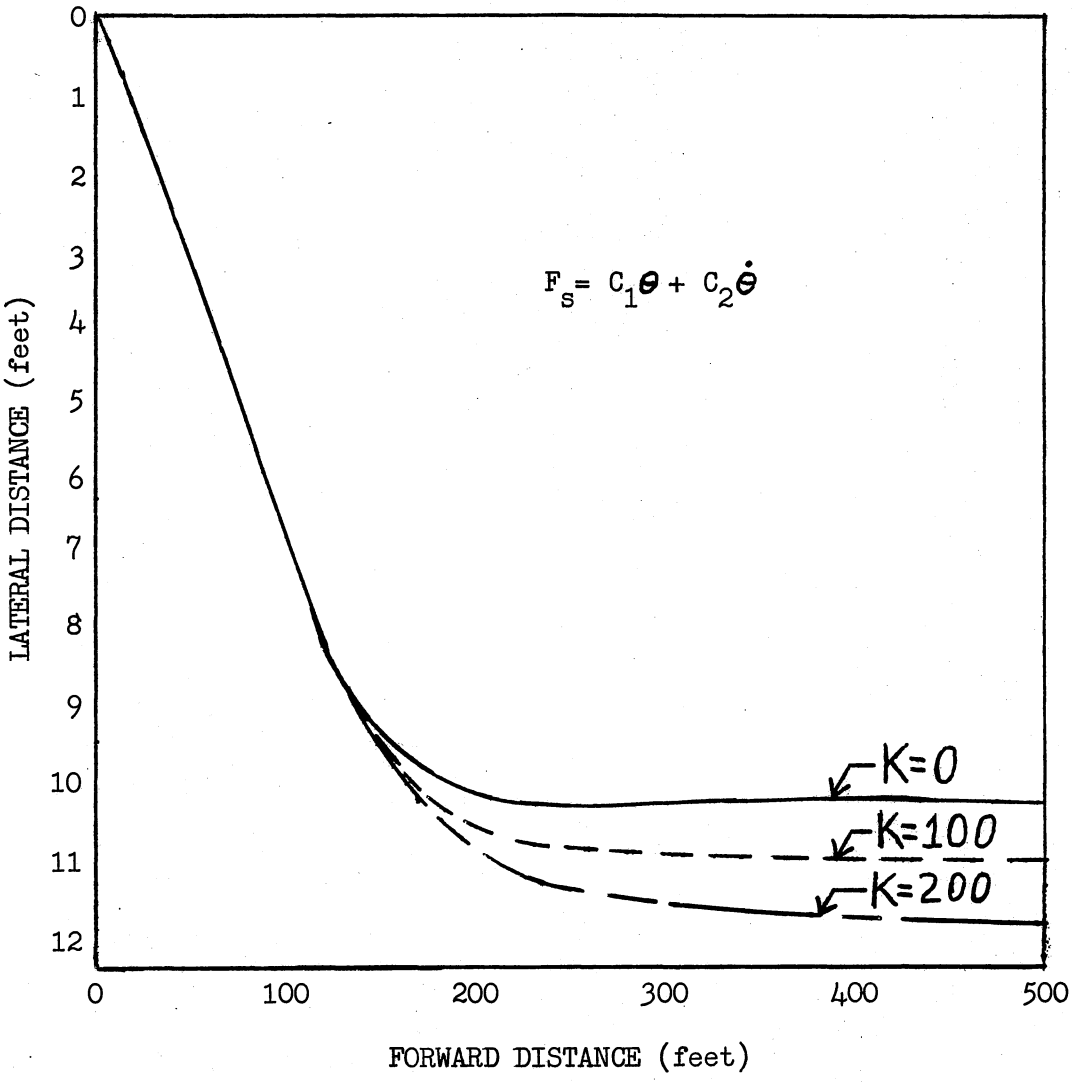

Figure 22. C.G. Travel Showing Oversteer Due to Stabilizer

1.6 ft might be critical for a narrow shoulder or a drop-off in the pavement. It can be concluded from this study that "oversteering" may result from the installation of a centering-type steering stabilizer.

CHAPTER V

SUMMARY, CONCLUSIONS AND RECOMMENDATIONS

This study has been made to develop an analytical method for determining the effects of steering stabilizers on vehicle controlability. The model used for this research simulated a single front axle and a single rear axle vehicle with the weight and dimensions chosen to be roughly equivalent to that of a typical tractor-truck. Application of Newton's Laws of motion to the body yielded the equations of motion and this set of equations was solved numerically using the Oklahoma State University IBM 360/65 computer.

Investigations were made for one particular type of stabilizing device to illustrate the capabilities of the method of analysis employed in this research and to gain physical insight into the significant effects of stabilizing devices. The major steps taken in this study are presented below.

1. Equations of motion were derived for a four-degree-of-freedom vehicle moving in a plane parallel with the horizontal roadway.

2. A numerical solution was obtained for the set of equations using DYSIMP and an auxiliary "table look-up" subroutine.

3. The validity of the computer program was verified by comparing with results for several simple cases in which the trends of response were known.

4. Three different driving situations were investigated to determine the effects of a steering stabilizer on the overall vehicle response.

The observations and conclusions made from this study are listed here.

1. The method of analysis (and the associated computer program) developed to study the effects of steering stabilizer devices on the vehicle response provided results that were physically reasonable for the cases studied.

2. Although a simple vehicle model was used, the technique can be readily extended to more complex systems.

3. During blowouts and sudden forces applied to the front wheels, a stabilizer will decrease the lateral distance traveled by the vehicle C.G. Given the proper situation this distance could be sufficient to prevent an accident.

4. The steering force, which is proportional to the driver input force, required to control the vehicle during a sudden force on the front wheels was decreased by using a stabilizing device. Not only was the maximum value less, but also the force required over the entire restoring time interval gradually decreased. Thus, less effort was supplied by the driver.

5. The driver reaction time used in this study was estimated to be $1\frac{1}{8}$ seconds. The actual time will vary between drivers and will depend upon the situation. However, this device produces a restoring force the instant the front wheel is displaced (i.e., it reacts "passively"). Therefore, a spring device will supply a restoring force during the reaction time interval of the driver.

6. Because the stabilizing device tends to keep the vehicle traveling in a straight path, it may produce harmful effects when a change in direction is desired. Results of this study indicated that oversteering will occur due to the presence of the spring device and may be expected to cause an increase in the lateral distance traveled by the vehicle C.G., thus allowing the vehicle to enter an unsafe region. Therefore, the spring device may create undesirable effects when the vehicle is being manuevered.

7. The spring device causes a significant increase in the required steering force when a large rotation of the front wheels is desired. For sharp turns, backing-up, and other slow maneuvers, the wheel may often be rotated as much as 40 degrees. To turn the wheels the driver must supply enough force to overcome the restoring moment, thus creating another undesirable effect from the spring device.

Recommendations for further study concerning this research are given as follows.

1. Experimental studies should be made to correlate results from the computer program with those experienced in real-life situations. This would allow the computer program to be used as a useful design tool and also to provide a dynamic simulation for the investigation of accidents.

2. The vehicle model should be extended to include one and two trailers. Jackknifing (a common problem for articulated vehicles) could then be analyzed by this model.

3. A study should be made to determine a more accurate transfer function to describe the driver response.

4. For this research the center of mass for the front wheels was assumed to lie on a vertical line passing through the point of tire contact with the road. It should be determined if a significant change occurs by moving the center of mass to a point between the king pin axis and the point of contact.

5. Both front wheels were assumed to rotate the same amount. However, the two wheels may actually rotate to slightly different angles and an investigation should be made to determine the effects this difference has on the vehicle response.

6. Camber in the front wheels should be studied to determine the restoring moment due to the camber angle, the maximum allowable angle, and the effects of combining a steering stabilizer with different camber angles.

7. A single rear axle was used for this research model. The model should be extended to include tandem axles each with dual tires.

8. A study should be made to determine more accurately the forces experienced by the front wheels during blowouts and other situations which are of interest.

9. The method of applying the braking forces should be improved so as to better simulate the actual driver application of braking forces for given situations.

BIBLIOGRAPHY

[1] Goland, M. and F. Jindra. "Car Handling Characteristics." Automobile Engineer, Vol. 50-51 (1960-61), pp. 296-302.

[2] Segel, Leonard. "On the Lateral Stability and Control of the Automobile as Influenced by the Dynamics of the Steering System." ASME Transactions, Vol. 88 (1966), pp. 283-293.

[3] Ellis, J. R. "Understeer and Oversteer." Automobile Engineer, Vol. 53 (1963), pp. 178-182.

[4] Weir, D. H. and D. T. McRuer. "Dynamics of Driver Vehicle Steering Control." Automatica, Vol. 6 (1970), pp. 87-98.

[5] Jindra, F. "Tractor and Semi-Trailer Handling." Automobile Engineer, Vol. 53 (1963), pp. 438-446.

[6] Ellis, J. R. "The Ride and Handling of Semi-Trailer Articulated Vehicles." Automobile Engineer, Vol. 56 (1966), pp. 523-529.

[7] Mikulcik, E. C. "The Dynamics of Tractor-Semitrailer Vehicles: The Jackknifing Problem." SAE Transactions, Vol. 80 (1971), paper 710045.

[8] Vincent, R. J. and A. I. Krauter. "Tractor-Semitrailer Handling: A Dynamic Tractor Suspension Model." SAE Transactions, Vol. 82 (1973), paper 730653.

[9] Jindra, F. "Tractor and Trailer Handling." Automobile Engineer, Vol. 55 (1965), pp. 60-70.

[10] Schmid, I. "Engineering Approach to Truck and Tractor Train Stability." SAE Transactions, Vol. 76 (1968), paper 670006.

[11] Hazemoto, T. "Analysis of Lateral Stability for Doubles." SAE Transactions, Vol. 82 (1973), paper 730688.

[12] Ginn, J. L. and R. L. Marlowe. "Road Contact Forces of Truck Tires as Measured in the Laboratory." SAE Transactions, Vol. 76 (1967), paper 670493.

[13] Nordeen, D. L. "Analysis of Tire Lateral Forces and Interpretation of Experimental Tire Data." SAE Transactions, Vol. 76 (1967), paper 670173.

[14] Dugoff, H. and R. W. Murphy. "The Dynamic Performances of Articulated Highway Vehicles--A Review of the State-of-the-Art." SAE Transactions, Vol. 80 (1971), paper 710223.

[15] Ebbesen, L. R. "DYSIMP User's Guide." (Unpublished manual, Oklahoma State University, 1975.)

[16] Kohno, T., S. Tsuchiya, and N. Komoda. "On the Vehicle Dynamic Response to the Steering Control." SAE Transactions, Vol. 77 (1969), paper 690488.

[17] Nix, J. C. "High Speed Table Lookup Subroutine." Gun Error Analysis/Advanced Control Systems. Final Report Contract No. 33615-72-C-2095. USAF/AFAL: Wright Patterson AFB, Ohio, December, 1972.

APPENDIX A

DERIVATION OF $\ddot{\bar{R}}_o$

The displacement of the origin (moving axis system x-y) with respect to the fixed reference system X-Y is given by

$$\bar{R}_o = R_x i + R_y j.$$

Thus, differentiation yields

$$\dot{\bar{R}}_o = \bar{V}_o = \dot{R}_x i + R_x \dot{i} + \dot{R}_y j + R_y \dot{j}. \tag{A.1}$$

Because i and j are unit vectors, then

$$\frac{di}{dt} = \dot{i} = \dot{\theta} j \tag{A.2}$$

$$\frac{dj}{dt} = \dot{j} = -\dot{\theta} i. \tag{A.3}$$

Substitution of i and j into Equation (A.1) yields

$$\dot{\bar{R}}_o = \dot{R}_x i + R_x \dot{\theta} j + \dot{R}_y \dot{j} - R_y \dot{\theta} \dot{j}$$

which can be simplified to yield

$$\dot{\bar{R}}_o = (\dot{R}_x - R_y \dot{\theta}) i + (\dot{R}_y + R_x \dot{\theta}) j.$$

Letting

$$\begin{aligned} U &= \dot{R}_x - R_y \dot{\theta} \\ V &= \dot{R}_y + R_x \dot{\theta} \\ r &= \dot{\theta} \end{aligned} \tag{A.4}$$

$\dot{\bar{R}}_o$ can be expressed as

$$\dot{\bar{R}}_o = \bar{V}_o = Ui + Vj.$$

Differentiating the above equation results as

$$\ddot{\bar{R}}_o = \bar{a}_o = \dot{U}i + U\dot{i} + \dot{V}j + V\dot{j}.$$

Using Equations (A.2), (A.3) and (A.4) yield

$$\ddot{\bar{R}}_o = \bar{a}_o = (\dot{U} - V\cdot r)i + (\dot{V} + U\cdot r)j. \qquad (A.5)$$

APPENDIX B

DERIVATION OF THE FRONT WHEEL C.G. ACCELERATION

The centers of gravity for the left and right front wheels are denoted as P_1 and P_2, respectively. Reference should be made to Figures 1 and 3. A detailed development will be given here for the acceleration of point P_2. The position of P_2 can be written vectorally as

$$\bar{R}_{p2} = \bar{R}_o + \bar{\rho}_1 + \bar{\rho}_2$$

where $\bar{R}_o$, $\bar{\rho}_1$ and $\bar{\rho}_2$ are defined as

$$\bar{R}_o = R_x i + R_y j$$

$$\bar{\rho}_1 = ai + \frac{1}{2} dj$$

$$\bar{\rho}_2 = -e \sin\delta i + e \cos\delta j.$$

Differentiating the expression of $\bar{R}_{p2}$ yields

$$\dot{\bar{R}}_{p2} = \dot{\bar{R}}_o + \dot{\bar{\rho}}_1 + \dot{\bar{\rho}}_2. \tag{B.1}$$

The terms for $\dot{\bar{\rho}}_1$ and $\dot{\bar{\rho}}_2$ can be expressed as

$$\dot{\bar{\rho}}_1 = a\dot{i} + \frac{1}{2} d\dot{j} \tag{B.2}$$

$$\dot{\bar{\rho}}_2 = (-e\,\dot{\delta}\cos\delta)i - (e \sin\delta)\dot{i} - (e\,\dot{\delta}\sin\delta)j + (e \cos\delta)\dot{j}. \tag{B.3}$$

Substituting $\dot{i} = \dot{\theta}j$ and $\dot{j} = -\dot{\theta}j$ into Equations (B.2) and (B.3) produces

$$\dot{\bar{\rho}}_1 = -\frac{1}{2} d\dot{\theta}i + a\dot{\theta}j$$

$$\dot{\bar{\rho}}_2 = -e\,(\dot{\delta} + \dot{\theta})(\cos\delta i + \sin\delta j)$$

Substitution of the above expressions into Equation (B.1) yields

$$\dot{\bar{R}}_{p2} = \dot{\bar{R}}_o + \dot{\theta}(-\tfrac{1}{2} d\dot{i} + a\dot{j}) - e(\dot{\delta} + \dot{\theta})(\cos\delta i + \sin\delta j). \qquad (B.4)$$

Differentiating Equation (B.4) produces

$$\begin{aligned}\bar{R}_{p2} = \bar{a}_{p2} = \bar{R}_o &+ \theta(-\tfrac{1}{2} d\dot{i} + a\dot{j}) + \dot{\theta}(-\tfrac{1}{2} d\dot{i} + a\dot{j}) \\ &- e(\delta + \theta)(\cos\delta i + \sin\delta j) - e(\dot{\delta} + \dot{\theta})(\cos\delta\dot{i} \\ &- \dot{\delta}\sin\delta i + \sin\delta\dot{j} + \dot{\delta}\cos\delta\dot{j}) \qquad (B.5)\end{aligned}$$

Defining $B = (\theta + \delta)$ and substituting into Equation (B.5) results as

$$\begin{aligned}\bar{a}_{p2} = \ddot{\bar{R}}_o &- \tfrac{1}{2} d\ddot{\theta} i + a\ddot{\theta} j - \tfrac{1}{2} d\dot{\theta}^2 j - a\dot{\theta}^2 i - e\ddot{\beta}(\cos\delta i + \sin\delta j) \\ &- e\dot{\beta}(\dot{\theta}\cos\delta j - \dot{\delta}\sin\delta i - \dot{\theta}\sin\delta i + \dot{\delta}\cos\delta\dot{j}) \qquad (B.6)\end{aligned}$$

Using the expression for $\ddot{\bar{R}}_o$ derived in Appendix A and collecting terms yields

$$\begin{aligned}\bar{a}_{p2} = &(e\dot{\beta}^2 \sin\delta - e\ddot{\beta}\cos\delta - \tfrac{1}{2} d\ddot{\theta} - a\dot{\theta}^2 + \dot{U} - V\cdot r)i \\ &- (e\dot{\beta}^2 \cos\delta + e\ddot{\beta}\sin\delta + \tfrac{1}{2} d\dot{\theta}^2 - a\ddot{\theta} - \dot{V} + U\cdot r)j. \qquad (B.7)\end{aligned}$$

The expression for $\bar{a}_{p1}$ is derived in a similar manner. Displacement of P_1 may be expressed as

$$\bar{R}_{p1} = \bar{R}_o + \bar{\rho}_3 + \bar{\rho}_4$$

where

$$\bar{\rho}_3 = ai + \tfrac{1}{2} dj$$

$$\bar{\rho}_4 = e\sin\delta i - e\cos\delta j$$

Repeating the procedure for $\bar{a}_{p2}$ with these two changes yields

$$\begin{aligned}\bar{a}_{p1} = &(-e\dot{\beta}^2 \sin\delta + e\ddot{\beta}\cos\delta + \tfrac{1}{2} d\ddot{\theta} - a\dot{\theta}^2 + \dot{U} - V\cdot r)i \\ &+ (e\dot{\beta}^2 \cos\delta + e\ddot{\beta}\sin\delta + a\ddot{\theta} + \tfrac{1}{2} d\dot{\theta}^2 + \dot{V} + U\cdot r)j \\ &\qquad (B.8)\end{aligned}$$

APPENDIX C

DERIVATION OF THE $\ddot{\beta}$ EQUATION

The equations of motion for the left wheel are

$$m_{w1}\, a_{p1y} = R_{y1} + F_{s1} + F_{y1}\cos\delta + F_{x1}\sin\delta \tag{C.1}$$

$$m_{w1}\, a_{p1x} = R_{x1} - F_{y1}\sin\delta + F_{x1}\cos\delta \tag{C.2}$$

$$I_{w1}\,\ddot{\beta}_1 = -K\delta - F_{s1}\,(S\cos\delta + e\sin\delta) - R_{y1}\, e\sin\delta - R_{x1}\, e\cos\delta. \tag{C.3}$$

Solving Equations (C.1) and (C.2) for R_{y1} and R_{x1}, then substituting into Equation (C.3) yields

$$I_{w1}\,\ddot{\beta}_1 = -K\delta - m_{w1}\, e(a_{p1y}\sin\delta + a_{p1x}\cos\delta) - S\,F_{s1}\cos\delta + eF_{x1}. \tag{C.4}$$

Using the components of $\bar{a}_{p1}$ expressed as

$$a_{p1x} = e(-\dot{\beta}^2\sin\delta + \ddot{\beta}\cos\delta + \frac{1}{2}\frac{d}{e}\dot{r} - \frac{1}{2}\frac{a}{e}r^2) + \dot{U} - V\cdot r$$

and

$$a_{p1y} = e(\dot{\beta}^2\cos\delta + \ddot{\beta}\sin\delta + \frac{a}{e}\dot{r} + \frac{1}{2}\frac{d}{e}r^2) + \dot{V} + U\cdot r$$

and substituting into Equation (C.4) results in

$$\ddot{\beta}_1 = \frac{1}{I_{w1} + m_{w1}\, e^2}\{-K\delta - m_{w1}\, e(\frac{1}{2}\, d\cos\delta + a\sin\delta)\dot{r} + m_{w1}\, e(a\cos\delta - \frac{1}{2}\, d\sin\delta)r^2 - S\,F_{s1}\cos\delta + e\,F_{x1} - m_{w1}\, e[(\dot{V} + U\cdot r)\sin\delta + (\dot{U} - V\cdot r)\cos\delta]\}. \tag{C.5}$$

The equations of motion for the right wheel are

$$m_{w2}\, a_{p2y} = R_{y2} + F_{s2} + F_{x2} \sin\delta + F_{y2} \cos\delta$$

$$m_{w2}\, a_{p2x} = R_{x2} + F_{x2} \cos\delta - F_{y2} \sin\delta$$

$$I_{w2}\, \ddot{\beta}_2 = -K\delta - F_{s2} (s \cos\delta - e \sin\delta) + R_{x2}\, e \cos\delta + R_{y2}\, e \sin\delta.$$

Repeating the previous procedure using

$$a_{p2y} = -e(\dot{\beta}^2 \cos\delta + \ddot{\beta} \sin\delta - \frac{a}{e} \dot{r} + \frac{1}{2} \frac{d}{e} r^2) + \dot{V} + U \cdot r$$

and

$$a_{p2x} = e(\dot{\beta}^2 \sin\delta - \ddot{\beta} \cos\delta - \frac{1}{2} \frac{d}{e} \dot{r} - \frac{a}{e} r^2) + \dot{U} - V \cdot r$$

results in

$$\ddot{\beta}_2 = \frac{1}{I_{w2} + m_{w2} e^2} \{-K\delta - F_{s2}\, s \cos\delta - F_{x2} e + m_{w2}\, e[\dot{r}(a \sin\delta - \frac{1}{2} d \cos\delta) - r^2 (a \cos\delta + \frac{1}{2} d \sin\delta) + (\dot{U} - V \cdot r) \cos\delta + (\dot{V} + U \cdot r) \sin\delta]\} \qquad (C.6)$$

Assuming that $m_{w1} = m_{w2}$, $I_{w1} = I_{w2}$, $\ddot{\beta}_1 = \ddot{\beta}_2$ and thus equating Equations (C.5) and (C.6) yield the following expression

$$(F_{s2} - F_{s1})\, s \cos\delta = -e(F_{x1} + F_{x2}) + 2m_w\, e[a(\dot{r} \sin\delta - r^2 \cos\delta) + (\dot{U} - V_r) \cos\delta + (\dot{V} + U_r) \sin\delta. \qquad (C.7)$$

Introducing the requirements that

$$F_s = F_{s1} + F_{s2} \qquad (C.8)$$

and combining Equations (C.7) and (C.8) yields

$$F_{s2}\ (s\ \cos\delta) = \frac{1}{2} F_s\ s\ \cos\delta - \frac{1}{2} e(F_{x1} + F_{x2})$$

$$+ m_w\ e[a(\dot{r}\ \sin\delta - r^2\ \cos\delta)$$

$$+ (\dot{V} + U \cdot r)\ \sin\delta + (\dot{U} - V \cdot r)\ \cos\delta] \qquad (C.9)$$

Substitution of Equation (C.9) into (C.6) gives the desired expression for $\ddot{\beta}$ in terms of F_s.

$$\ddot{\beta} = \frac{1}{I_w + m_w e^2} \{-K\delta - \frac{1}{2} F_s\ s\ \cos\delta + \frac{1}{2} e(F_{x1} - F_{x2})$$

$$- m_w\ e[\frac{1}{2} d(\dot{r}\ \cos\delta + r^2\ \sin\delta)]\} \qquad (C.10)$$

APPENDIX D

DERIVATION OF REAR SLIP ANGLE

From Figures 1 and 3, $\bar{R}_q$ is expressed as

$$\bar{R}_q = \bar{R}_o + \bar{R}_2 \tag{D.1}$$

where

$$\bar{R}_o = R_x i + R_y j \tag{D.2}$$

$$\bar{R}_2 = -bi + \frac{1}{2} wj. \tag{D.3}$$

Differentiating Equations (D.1), (D.2) and (D.3) yields

$$\dot{\bar{R}}_q = \dot{\bar{R}}_o + \dot{\bar{R}}_2$$

$$\dot{\bar{R}}_o = \dot{R}_x i + R_x \dot{i} + \dot{R}_y j + R_y \dot{j} \tag{D.4}$$

$$\dot{\bar{R}}_2 = -b\dot{i} + \frac{1}{2} w\dot{j}. \tag{D.5}$$

Because $\dot{i} = rj$ and $\dot{j} = -ri$ and substituting these expressions into Equations (D.4) and (D.5) yield

$$\dot{\bar{R}}_o = (\dot{R}_x - rR_y)i + (\dot{R}_y + rR_x)j$$

and

$$\dot{\bar{R}}_2 = -\frac{1}{2} wri - brj$$

$\dot{\bar{R}}_q$ is now expressed as

$$\dot{\bar{R}}_q = (\dot{R}_x - rR_y - \frac{1}{2} wr)i + (\dot{R}_y + rR_x - br)j.$$

The angle between $\dot{\bar{R}}_q$ and the wheel heading (unit vector in the i direction) is the rear slip angle (α_r). Using the definition for the dot

product,

$$\overline{A} \cdot \overline{B} = |AB| \cos\alpha \tag{D.6}$$

and letting

$$\overline{A} = i$$

$$\overline{B} = \dot{\overline{R}}_p$$

Equation (D.6) becomes

$$i \cdot \dot{\overline{R}}_p = |\dot{\overline{R}}_p| \cos\alpha_r$$

thus

$$\alpha_r = \text{Arc cos } \left(\frac{R_{qx}}{\sqrt{R_{qx}^2 + R_{qy}^2}}\right) \tag{D.7}$$

where

$$R_{qx} = \dot{R}_x - r R_y - \frac{1}{2} w r$$

and

$$R_{qy} = \dot{R}_y + r R_x - b r.$$

The sign of α_r is equal to the sign of R_{qy}.

VITA

David Lynn Turney

Candidate for the Degree of

Master of Science

Thesis: A PRELIMINARY STUDY OF THE EFFECTS OF FRONT WHEEL STEERING STABILIZERS ON VEHICLE RESPONSE CHARACTERISTICS

Major Field: Mechanical Engineering

Biographical:

Personal Data: Born February 18, 1951, in Heber Springs, Arkansas, the son of Mr. and Mrs. R. L. Turney.

Education: Graduated from Quitman High School, Quitman, Arkansas, in May, 1969; received the Degree of Bachelor of Science in Mechanical Engineering in 1973 from Louisiana Tech University; completed the requirements for the Degree of Master of Science at Oklahoma State University in May, 1975.

Professional Experience: Graduate Teaching Assistant, Oklahoma State University, 1973-1975.

Professional Organizations: Tau Beta Pi, Pi Tau Sigma, Phi Kappa Phi.